

# ChemComm

Chemical Communications

Accepted Manuscript

This article can be cited before page numbers have been issued, to do this please use: P. Kushwaha, A. Saxena, T. von Münchow, S. Dana, B. Saha and L. Ackermann, *Chem. Commun.*, 2024, DOI: 10.1039/D4CC03871A.



This is an Accepted Manuscript, which has been through the Royal Society of Chemistry peer review process and has been accepted for publication.

Accepted Manuscripts are published online shortly after acceptance, before technical editing, formatting and proof reading. Using this free service, authors can make their results available to the community, in citable form, before we publish the edited article. We will replace this Accepted Manuscript with the edited and formatted Advance Article as soon as it is available.

You can find more information about Accepted Manuscripts in the [Information for Authors](#).

Please note that technical editing may introduce minor changes to the text and/or graphics, which may alter content. The journal's standard [Terms & Conditions](#) and the [Ethical guidelines](#) still apply. In no event shall the Royal Society of Chemistry be held responsible for any errors or omissions in this Accepted Manuscript or any consequences arising from the use of any information it contains.

# 1 Metallaelectro-catalyzed Alkyne Annulations via C–H Activations for 2 Sustainable Heterocycle Syntheses

3 Preeti Kushwaha<sup>1,2</sup>, Anjali Saxena<sup>2</sup>, Tristan von Münchow<sup>3</sup>, Suman Dana<sup>3</sup>, Biswajit Saha\*<sup>2</sup>, Lutz  
4 Ackermann\*<sup>3</sup>

5 <sup>1</sup>Amity Institute of Click chemistry Research & Studies, Amity University, Noida, 201303, Uttar Pradesh, India

6 <sup>2</sup>Amity Institute of Biotechnology, Amity University, Noida, 201303, Uttar Pradesh, India

7 <sup>3</sup>Wöhler Research Institute for Sustainable Chemistry (WISCh), Georg-August-Universität Göttingen, 37077,  
8 Göttingen, Germany

9 \**Corresponding authors: Biswajit Saha (bsahal@amity.edu), Lutz Ackermann (Lutz.Ackermann@chemie.uni-*  
10 *goettingen.de)*

## 12 Abstract

13 Alkyne annulation represents a versatile and powerful strategy for the assembly of structurally  
14 complex compounds. Recent advances successfully enabled electrocatalytic alkyne annulations,  
15 significantly expanding the potential applications of this promising technique towards sustainable  
16 synthesis. The metallaelectro-catalyzed C–H activation/annulation stands out as a highly efficient  
17 approach that leverages electricity, combining the benefits of electrosynthesis with the power of  
18 transition-metal catalyzed C–H activation. Particularly attractive is the pairing of the electro-  
19 oxidative C–H activation with the valuable hydrogen evolution reaction (HER), thereby addressing  
20 the growing demand for green energy solutions. Herein, we provide an overview of the evolution  
21 of electrochemical C–H annulations with alkynes for the construction of heterocycles, with a  
22 topical focus on the underlying mechanism manifolds.

23 **Keywords:** Electrosynthesis; Alkynes; Annulations; Heterocycles; Transition-metal catalysis;  
24 Hydrogen

25

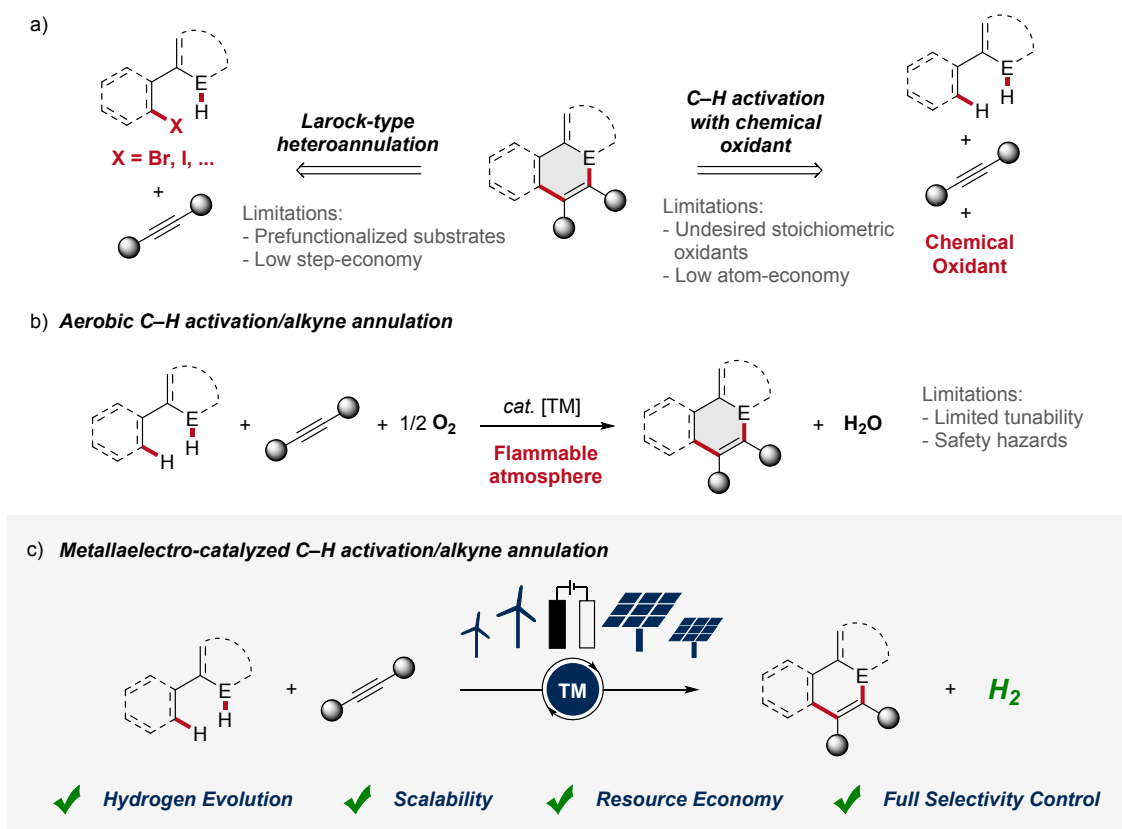


## 26 1 Introduction

27 Alkynes are key substrates in molecular synthesis. Due to their versatile reactivity, they enable a  
28 wide array of transformations, including cycloadditions, coupling reactions, and  
29 hydrofunctionalizations, among others.<sup>[1]</sup> Hence, access to compounds is provided that are  
30 essential for a broad spectrum of applications, ranging from material sciences to drug development  
31 and crop protection. In this context, the transition-metal catalyzed alkyne annulation is a powerful  
32 tool for the assembly of diverse heterocyclic compounds as it allows for the expedient construction  
33 of intricate molecular frameworks.<sup>[2]</sup> However, especially Larock-type heteroannulations face  
34 limitations, including the need for pre-functionalized substrates, expensive catalysts, and harsh  
35 reaction conditions. While alkyne annulations via C–H activation offer improvements in terms of  
36 step economy, significant obstacles remain, as the use of toxic heavy metal salts as oxidant is often  
37 involved. Consequently, these drawbacks have led to a strong demand for more sustainable  
38 strategies (**Figure 1a**). As a consequence, aerobic transition metal-catalyzed C–H activation was  
39 introduced for the construction of heterocycles, exhibiting improved atom economy with water as  
40 the sole byproduct (**Figure 1b**). Thus, in 2015, Ackermann described the aerobic ruthenium-  
41 catalyzed C–H annulation for the assembly of isocoumarins.<sup>[3]</sup> Despite of major advances, such  
42 oxidase catalysis had thus far been limited to toxic and expensive precious transition metals. In  
43 sharp contrast, in 2016, Ackermann reported on aerobic cobalt-catalyzed C–H alkyne annulations  
44 to access versatile isoquinolones.<sup>[4]</sup> While representing key progress, aerobic transition metal-  
45 catalysis was characterized by major drawbacks, including a) fixed redox potential with limited  
46 tunability,<sup>[5]</sup> b) safety hazards associated with the use of molecular oxygen with flammable  
47 solvents.<sup>[6]</sup> Thus, for industrial processes the limiting oxygen concentration (LOC), which defines  
48 the minimum partial pressure of oxygen that supports a combustible mixture, prohibits the broad  
49 implementation.<sup>[6]</sup> In contrast, the advent of metallaelectro-catalyzed C–H activation, which  
50 combines transition-metal catalyzed C–H activation and electrochemistry, offers an inherently safe  
51 and sustainable approach to construct valuable organic molecules (**Figure 1c**).<sup>[7]</sup> Importantly, this  
52 synergistic strategy offers a scalable approach to harness renewable forms of energy for a green  
53 hydrogen economy through the cathodic hydrogen evolution reaction (HER).<sup>[8]</sup> Whereas, in  
54 metallaelectro-catalyzed C–H activation electricity – protons and electrons – is employed as a  
55 “traceless-oxidant”, obviating the formation of stoichiometric waste generated from chemical



56 oxidants.<sup>[9]</sup> Herein, we thus summarize the rapid recent evolution of metalla-electrocatalysis for  
57 alkyne annulations until August 2024.



58

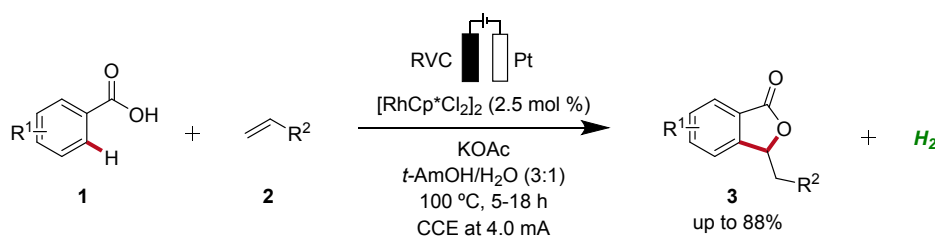
59 **Figure 1:** a) Common strategies for the assembly of heterocycles via alkyne annulation. b)  
60 Improved atom economy by aerobic C-H activation/annulation. c) Metallaelectro-catalyzed C-H  
61 activation/annulation as resource-economic approach. E = heteroatom. TM = transition metal.

62



63 **2 4d and 5d Metallalectro-Catalyzed Alkyne Annulations**64 **2.1 Rhodaelectro-Catalyzed C–H Activation**

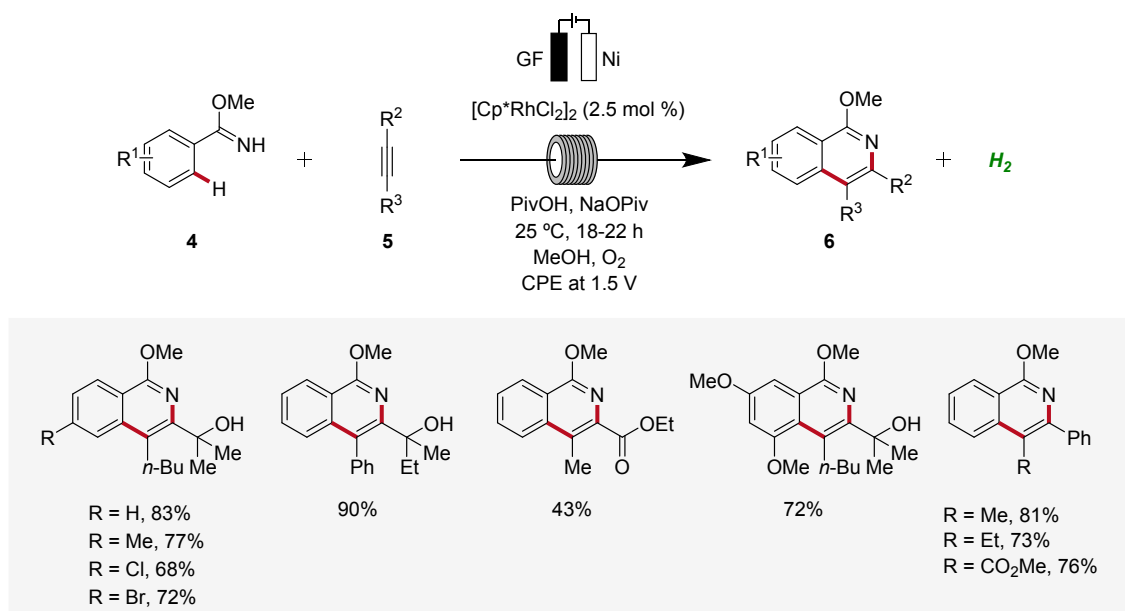
65 Rhodium catalysis represents a powerful and versatile approach to chemical synthesis, offering  
66 high efficiency and selectivity across a wide range of transformations.<sup>[10]</sup> Pioneering work in the  
67 field of rhodaelectro-catalyzed C–H activation was accomplished by Ackermann in 2018 (**Scheme**  
68 **1**).<sup>[11]</sup> Here, the electro-oxidative C–H activation of weakly coordinating benzoic acids **1** for the  
69 assembly of versatile isobenzofuranones **3** was described.



71 **Scheme 1:** Assembly of isobenzofuranones **3** enabled by the first rhodaelectro-catalyzed C–H  
72 activation.

73 Subsequently, in 2019, Ackermann established a user-friendly and scalable flow rhodaelectro-  
74 catalyzed alkyne annulation for the synthesis of isoquinolines **6** (**Scheme 2**).<sup>[12]</sup> The  
75 electrocatalysis proved amenable to differently substituted aryl imidates **4** under flow-  
76 electrochemical conditions. This electrocatalytic C–H/N–H alkyne annulation exhibited high  
77 levels of functional group tolerance and remarkable regioselectivity with unsymmetrical alkynes  
78 **5**. Moreover, the electro-flow approach was suitable for intramolecular C–H/N–H  
79 functionalization, providing direct access to azo-tetracycles.<sup>[12]</sup>



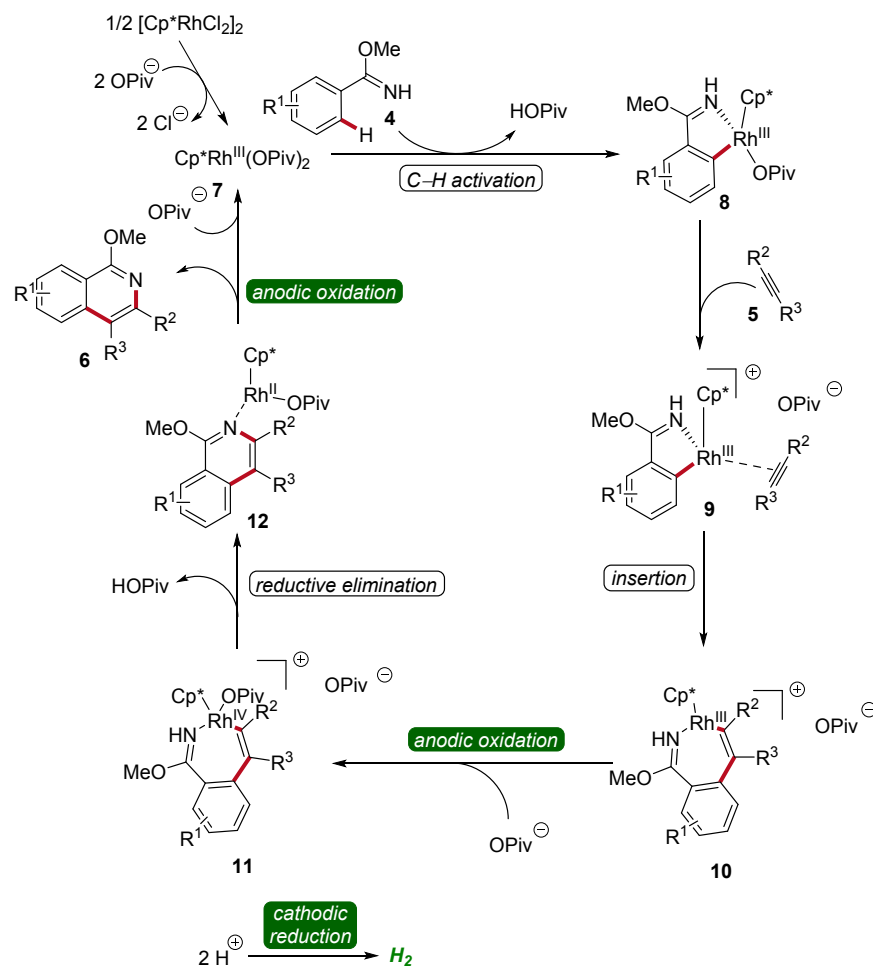


80

81 **Scheme 2:** Flow rhodaelectro-catalyzed alkyne annulations for the synthesis of isoquinolines **6**.

82 The mechanism of rhoda-electrocatalysis was investigated in detail, employing the isolation and  
 83 characterization of relevant organometallic intermediates, *in-operando* kinetic studies, cyclic  
 84 voltammetric investigations, and DFT analyses. Thus, the pre-catalyst  $[\text{Cp}^*\text{RhCl}_2]_2$  first undergoes  
 85 ligand exchange with NaOPiv to form the monomeric  $\text{Cp}^*\text{Rh}(\text{OPiv})_2$  **7**. This complex then is  
 86 coordinated by the imidate **4**, followed by the formation of the rhoda(III)-cycle **8** through C–H  
 87 activation. Subsequent coordination of the alkyne **5** and migratory insertion result in the generation  
 88 of the rhodium(III) heptacycle **10**. Under the electrochemical conditions, the formation of product  
 89 **6** is promoted by an oxidation-induced reductive elimination involving the anodic oxidation of the  
 90 rhoda(III)-cycle **10** to generate rhodium(IV) intermediate **11** (**Scheme 3**).<sup>[12]</sup>



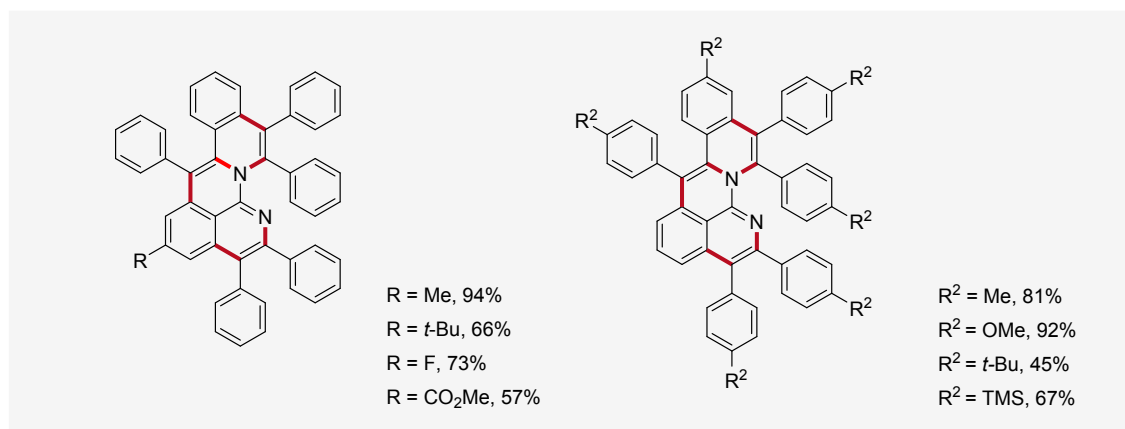
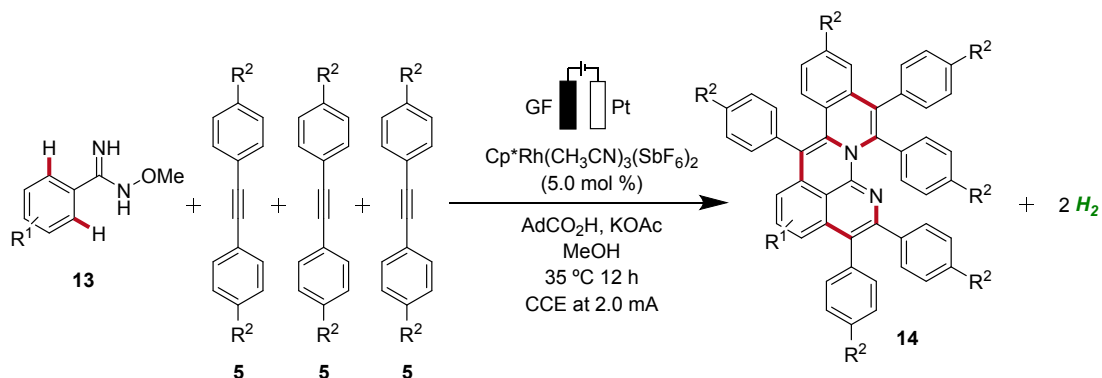


91

92 **Scheme 3:** Mechanism of flow rhodaelectro-catalyzed alkyne annulations for the synthesis of  
93 isoquinolines **6**.

94 In 2020, Ackermann reported an unique one-step electrochemical assembly of *aza*-polycyclic  
95 aromatic hydrocarbons **14** (*aza*-PAH) using rhodaelectro-catalyzed domino C–H annulations  
96 (**Scheme 4**).<sup>[13]</sup> The reaction of amidoximes **13** and alkynes **5** resulted in the desired *aza*-PAHs **14**  
97 via threefold C–H activations with high levels of regioselectivity. The feasibility of this  
98 electrocatalysis was proven by scalability, user-friendly setup, and mild reaction conditions.  
99 Hence, the electrocatalytic transformation was efficiently established in an undivided cell setup  
100 with ample scope and significant levels of functional group tolerance.<sup>[13]</sup>





101

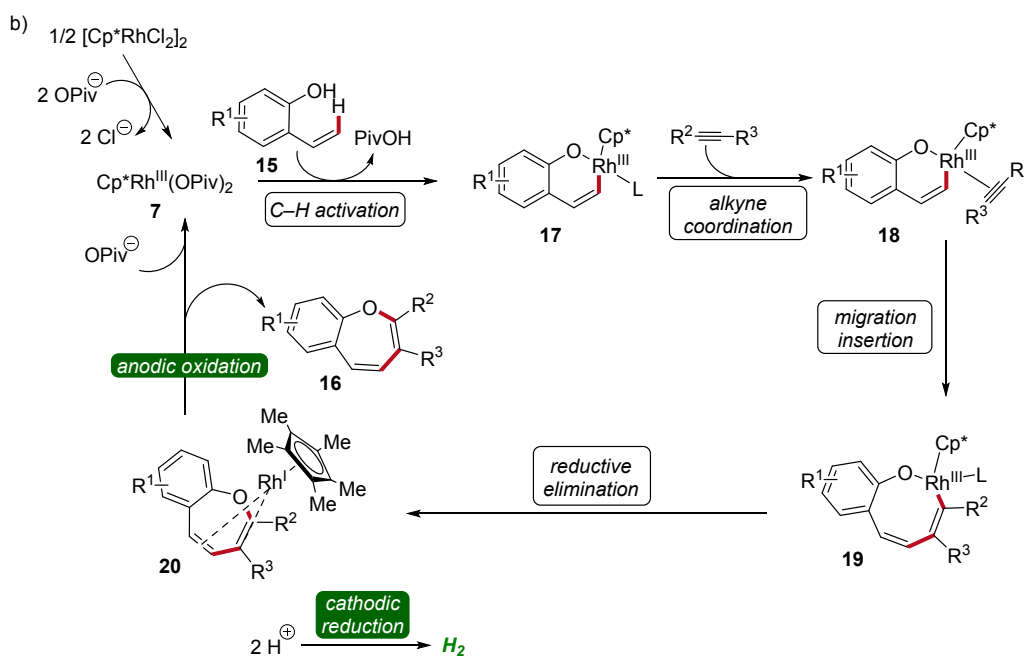
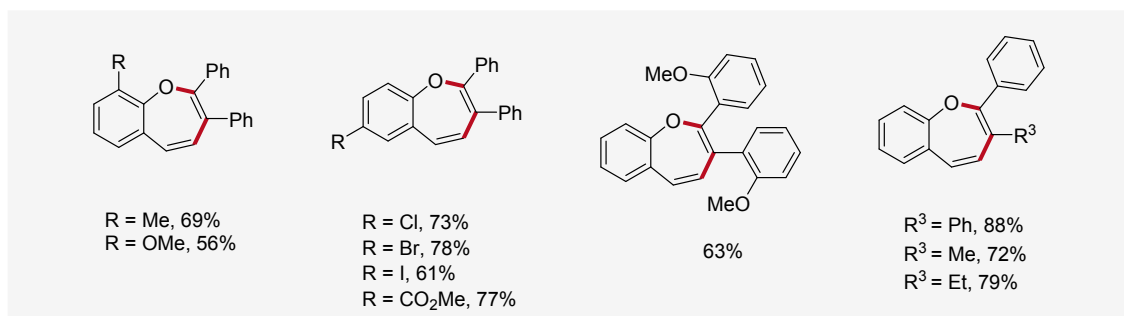
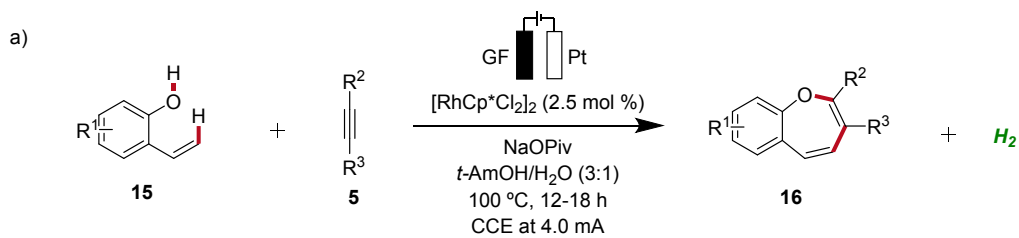
102 **Scheme 4:** Electrochemical synthesis of *aza*-polycyclic aromatic hydrocarbons **14** via  
103 rhodaelectro-catalyzed domino C–H annulations.

104 Recently, metallaelectro-catalyzed reactions have provided efficient routes for the constructions  
105 of various five- and six-membered heterocyclic ring structures via formal [3+2] or [4+2]  
106 cycloadditions.<sup>[14]</sup> In 2021, Ackermann reported the first rhodaelectro-catalyzed [5+2]  
107 cycloaddition reactions for the synthesis of benzoxepine motifs **16** using 2-vinylphenols **15** and  
108 alkynes **5** (**Scheme 5**).<sup>[15]</sup> This rhodium(III/I)-catalyzed annulation reaction was amenable to  
109 diversely functionalized 2-vinylphenols **15** and alkynes **5**, demonstrating a broad substrate scope  
110 and functional group tolerance. Detailed mechanistic studies revealed a facile C–H rhodation  
111 under a rhodium(III/I) regime. Furthermore, a benzoxepine-coordinated rhodium(I)sandwich  
112 complex **20** could be isolated, which could further be confirmed as a crucial intermediate of the  
113 devised electrocatalysis.<sup>[15]</sup>

114





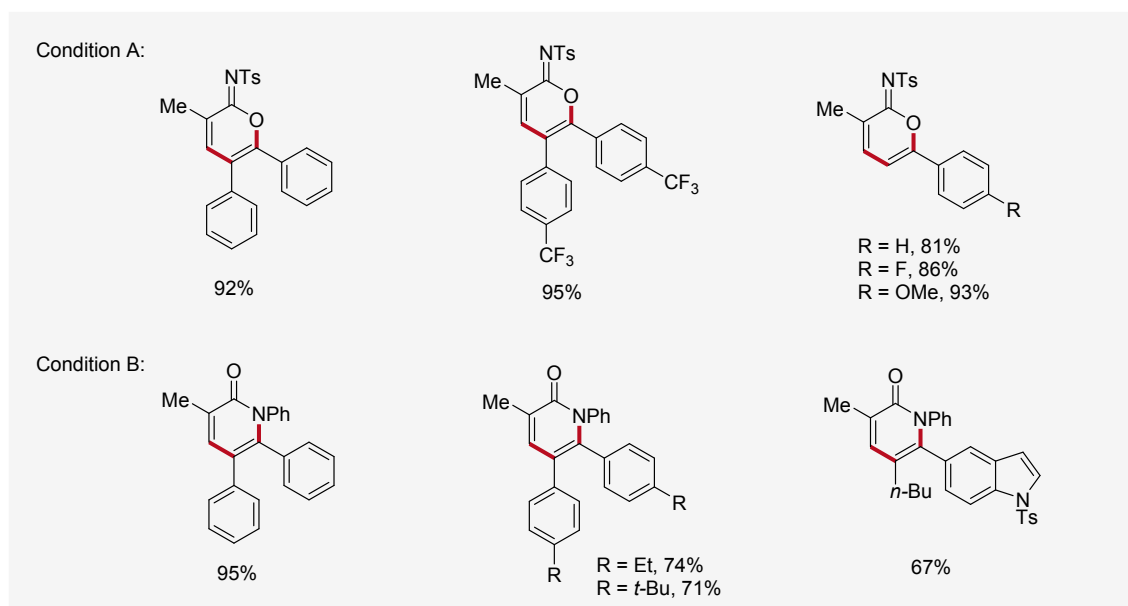
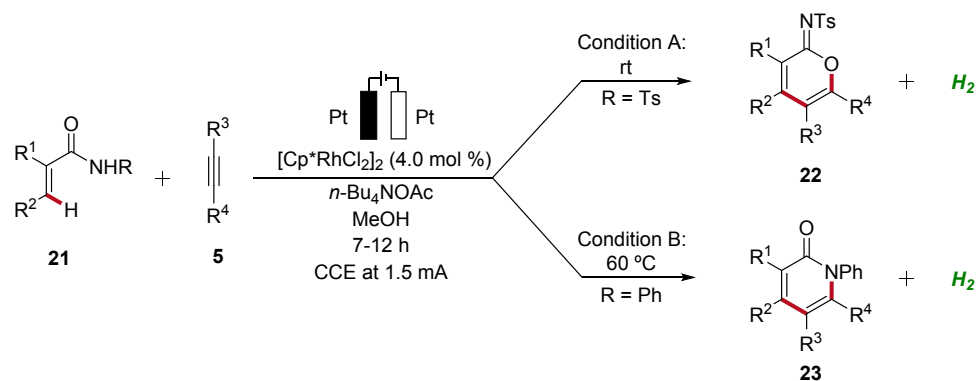


115

116 **Scheme 5:** Versatility and mechanism of the rhodaelectro-catalyzed synthesis of benzoxepines **16**.

117 In 2021, Mei established the vinylic C–H annulation of acrylamides **21** with alkynes **5** using  
 118 divergent rhodaelectro-catalysis (**Scheme 6**).<sup>[16]</sup> Various cyclic imidates **22** and  $\alpha$ -pyridones **23**  
 119 were synthesized by varying the *N*-substituent of acrylamides **21** in an undivided cell using mild  
 120 reaction conditions. The electrocatalysis proceeds for both reaction pathways with excellent  
 121 regioselectivity using unsymmetrical internal or terminal alkynes **5**.

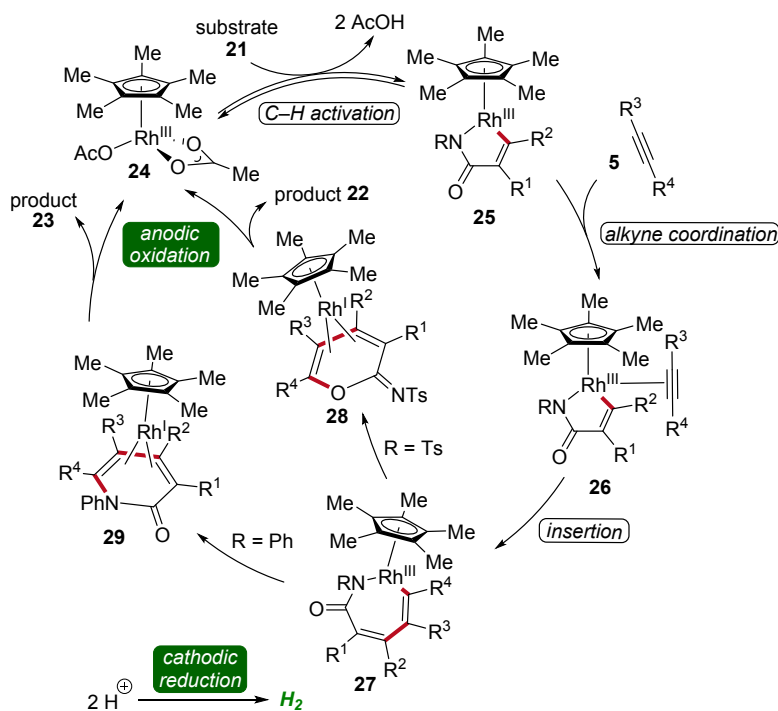




122  
123 **Scheme 6:** Synthesis of imidates **22** and  $\alpha$ -pyridones **23** enabled by divergent rhodaelectro-  
124 catalyzed vinylic C–H annulation.

125 Cyclic voltammetric analysis and kinetic isotopic effect studies have elucidated the mechanism of  
126 this rhodaelectro-catalyzed vinylic C–H annulation. The seven-membered rhoda(III)-cycle **27** is  
127 formed by C–H activation followed by insertion of alkyne **5**. This intermediate can undergo two  
128 distinct pathways: depending on the electronic nature of the *N*-substituent of the acrylamide **21**  
129 either an ionic stepwise pathway that generates intermediate **28**, which further yields the cyclic  
130 imidates **22**, or directly a reductive elimination, generating intermediate **29**, which leads to the  
131 formation of pyridones **23** takes place (**Scheme 7**).<sup>[16]</sup>





132

133 **Scheme 7:** Plausible catalytic cycle for the assembly of imidates **22** and  $\alpha$ -pyridones **23**.

134 In 2021, Ackermann developed a rhodaelectro-catalyzed formyl C–H activation (**Scheme 8**).<sup>[17]</sup>

135 This strategy enabled the direct synthesis of various chromones **31** from hydroxybenzaldehydes

136 **30**. Notably, despite benzaldehydes generally being considered oxidation-sensitive, the identified

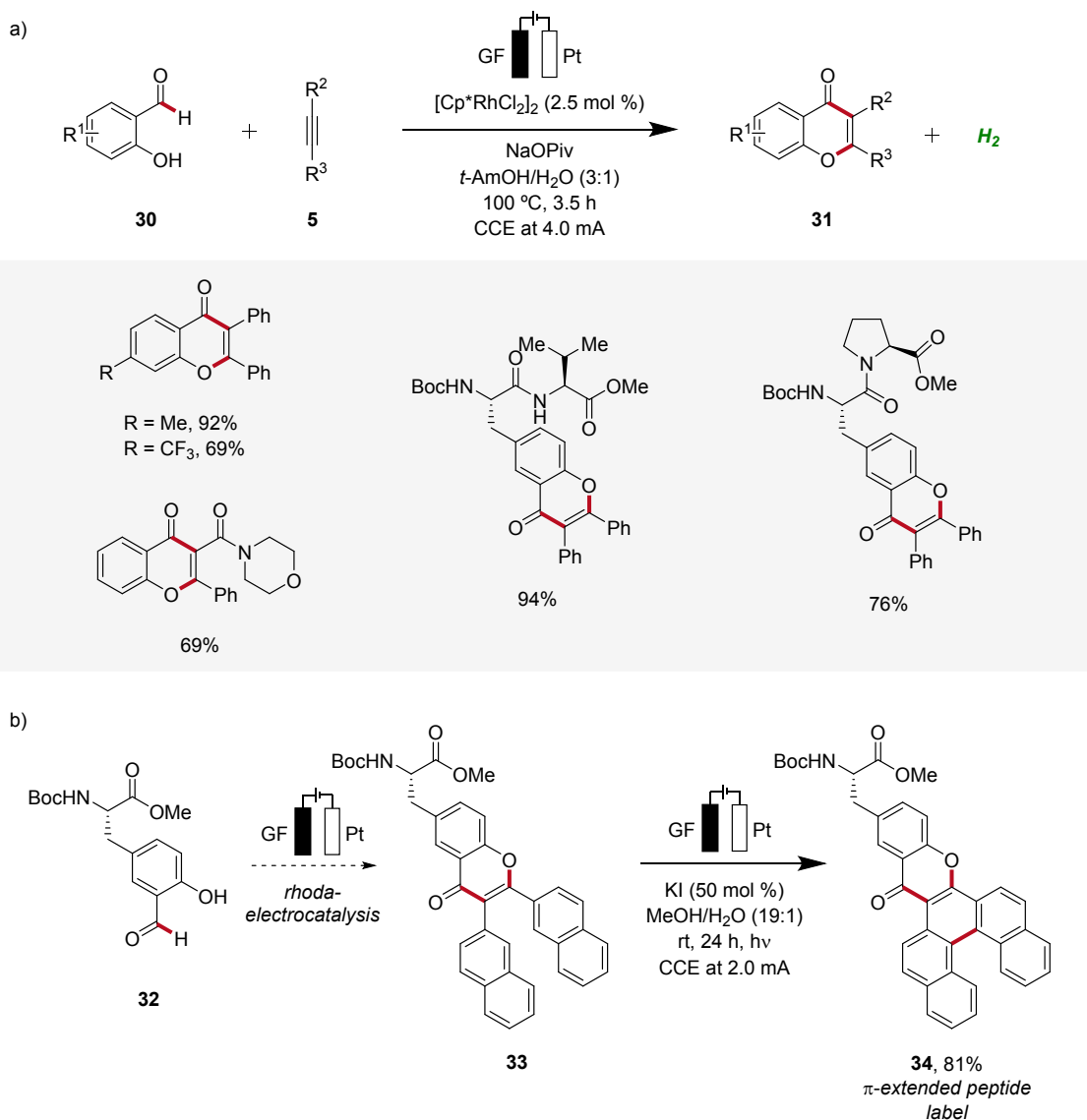
137 mild reaction conditions for the rhoda-electrocatalysis allowed for an applicability with a wide

138 range of substrates including peptides (**Scheme 8a**). Moreover, it was demonstrated that from the

139 obtained chromone **33**  $\pi$ -extended peptide labels **34** can be accessed through a

140 photoelectrochemical process (**Scheme 8b**).<sup>[17]</sup>



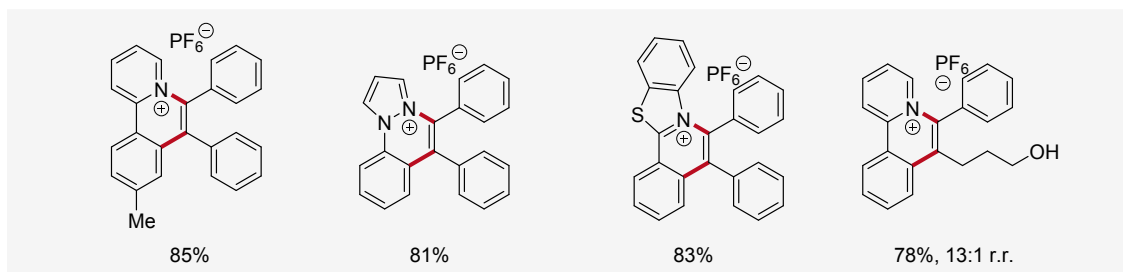
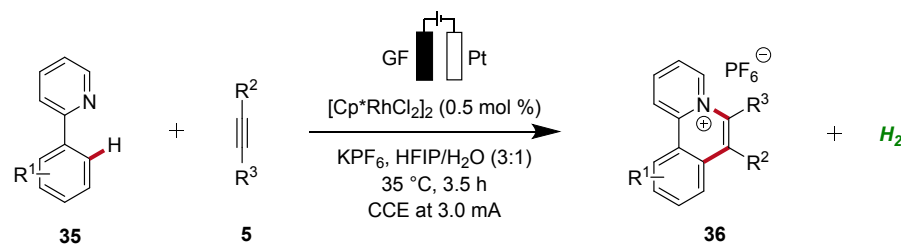


141

142 **Scheme 8:** Versatility of rhodaelectro-catalyzed alkyne annulations for the synthesis of chromones  
 143 **31** and its application to introduce fluorescent labels **34**.

144 In 2021, Zhang described a rhodaelectro-catalyzed C–H annulation for the construction of cationic  
 145 polycyclic heteroarenes **36** (Scheme 9).<sup>[18]</sup> Here, mechanistic studies, including the isolation of  
 146 organometallic intermediates and cyclic voltammetric analyses, were conducted. Additionally, the  
 147 regioselectivity in the annulation process was elucidated through detailed computational  
 148 studies.<sup>[18]</sup>





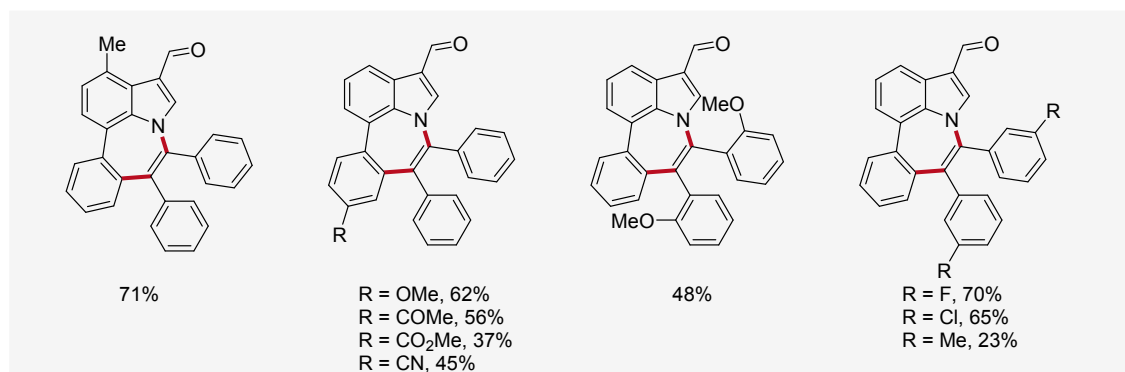
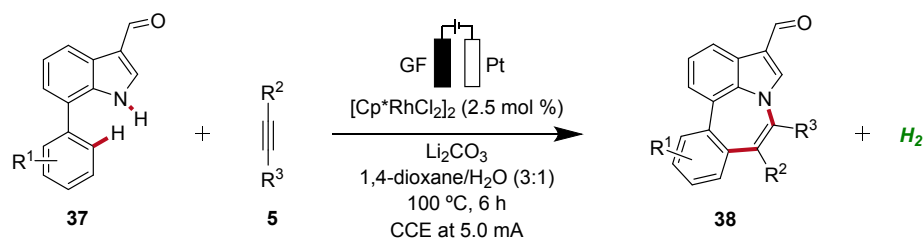
149  
150 **Scheme 9:** Rhodaelectro-catalyzed C–H annulation to construct cationic polycyclic heteroarenes  
151 **36.**

152 In 2022, Ackermann, Huang, and Ni reported a rhodaelectro-catalyzed [5+2] C–H/N–H annulation  
153 using 7-phenylindoles **37** with alkynes **5** in an undivided cell to construct azepino[3,2,1-*hi*]indoles  
154 **38** (Scheme 10).<sup>[19]</sup> This electrocatalysis exhibited a broad substrate scope with ample functional  
155 group tolerance and gram scalability through flow electrocatalysis. Thus, 7-phenylindoles **37**  
156 substituted at different positions as well as *ortho*-, *meta*-, or *para*-substituted diphenylacetylenes  
157 **5** proved to be compatible.<sup>[19]</sup>

158



159

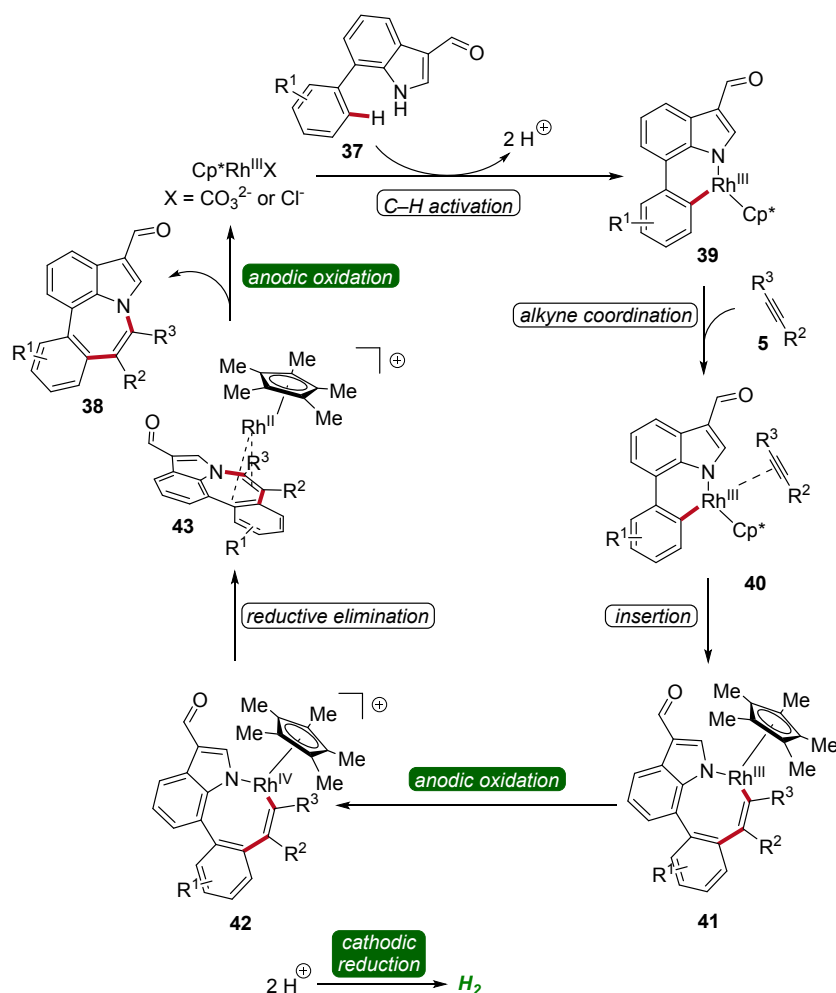


160

161 **Scheme 10:** Rhodaelectro-catalyzed [5+2] C–H/N–H annulation reaction for the construction of  
162 azepino[3,2,1-*hi*]indoles **38**.

163 A reaction mechanism was proposed derived from deuterium-labeling studies, cyclic voltammetric  
164 analyses, and X-ray photoelectron spectroscopy studies. Based on these findings, the formation of  
165 the six-membered rhoda(III)-cycle **39** through C–H activation was postulated. A migratory  
166 insertion with coordinated alkyne **5** then occurs, leading to the eight-membered rhoda(III)-cycle  
167 **41**. Finally, an oxidation-induced reductive elimination via a rhodium(III/IV/II) pathway facilitates  
168 the release of the azepino[3,2,1-*hi*]indole product **38** (Scheme 11).<sup>[19]</sup>



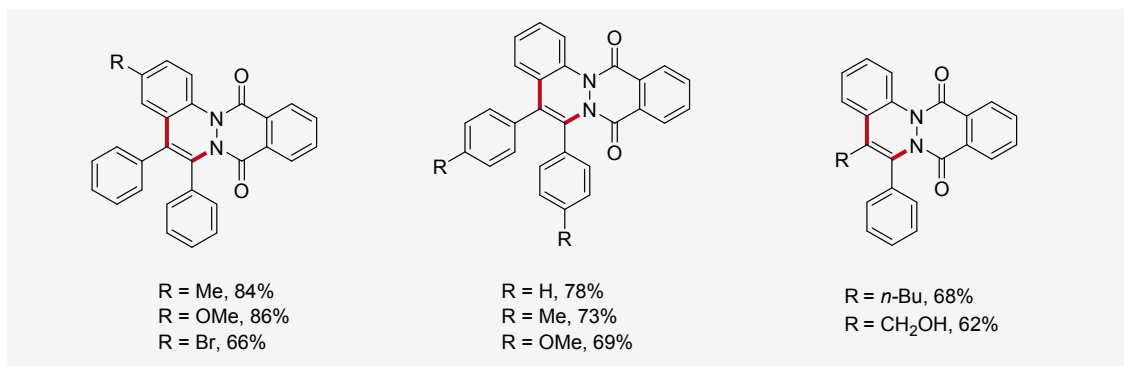
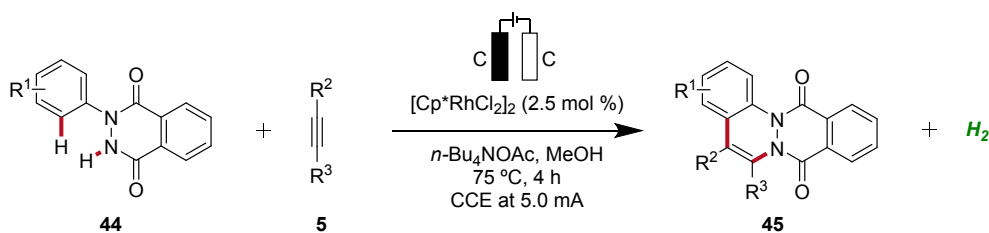


169

170 **Scheme 11:** Mechanism of rhodaelectro-catalyzed [5+2] C-H/N-H annulation reaction for the  
 171 assembly of azepino[3,2,1-*hi*]indoles **38**.

172 Similarly, in 2022, a rhodaelectro-catalyzed [4+2] C-H annulation was reported by Roy for the  
 173 synthesis of cinnolines **45** (**Scheme 12**).<sup>[20]</sup> The C-H/N-H annulation of  
 174 arylhydrophthalazinediones **44** with alkynes **5** using precatalyst  $[\text{Cp}^*\text{RhCl}_2]_2$  in an undivided cell  
 175 under galvanostatic conditions afforded efficiently the desired cinnolines **45**. The robustness and  
 176 versatility of the developed method was tested by employing diversely decorated 2-aryl-3-  
 177 hydrophthalazinediones **44** as well as symmetrical and unsymmetrical internal alkynes **5**, while  
 178 the desired products **45** were furnished in good to excellent yields. However, terminal alkynes  
 179 were not compatible. Cyclic voltammetry and differential pulse voltammetry experiments revealed  
 180 the formation of the annulated products **45** through a Rh(III/I) and Rh(III/IV) pathway.<sup>[20]</sup>





181

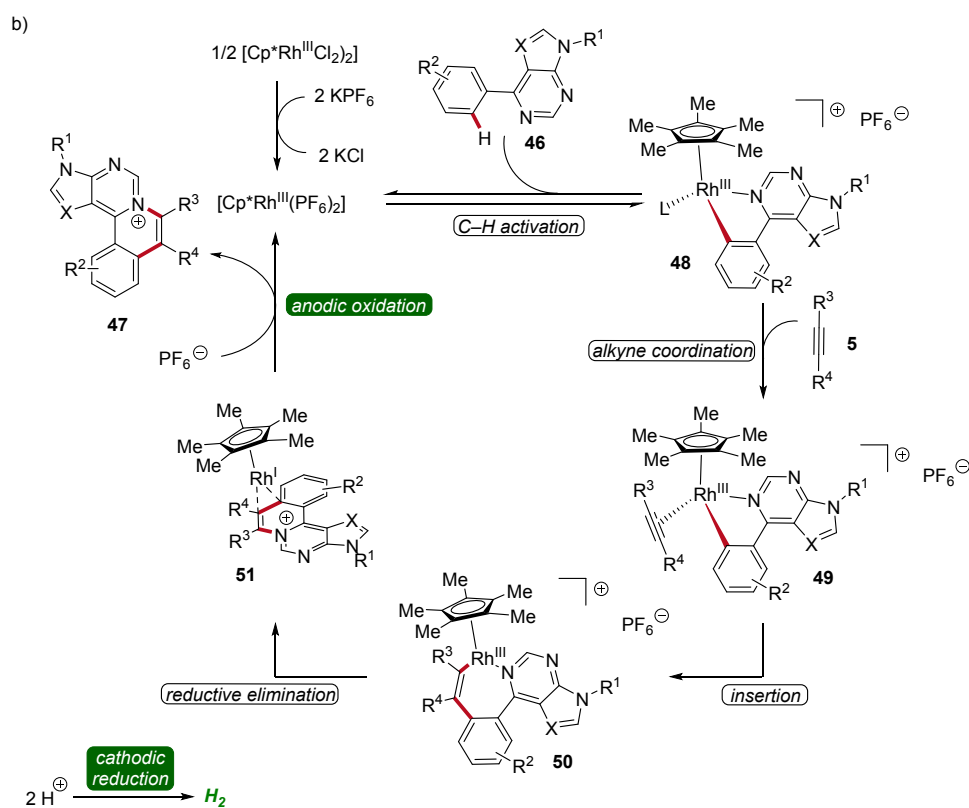
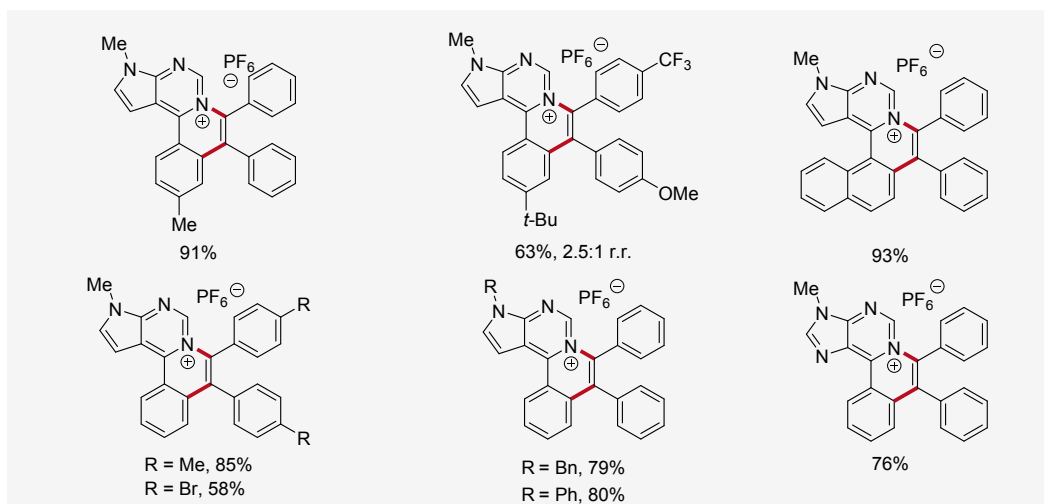
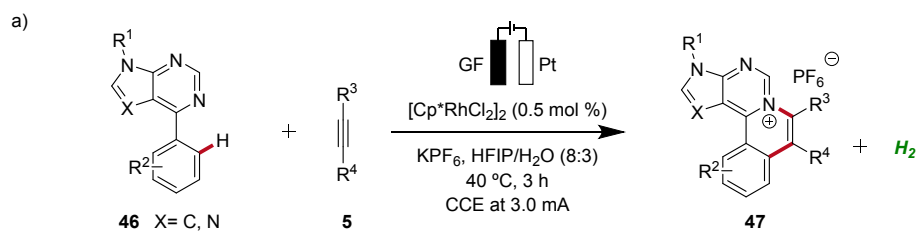
182 **Scheme 12:** Rhodaelectro-catalyzed C-H/N-H annulation for the synthesis of cinnolines **45**.

183 Likewise, a rhodaelectro-catalyzed [4+2] C-H activation/annulation with internal alkynes **5** was  
 184 reported by Ling in 2022 (**Scheme 13**).<sup>[21]</sup> This expedient strategy provided a new series of  
 185 polycyclic (7-deaza)purinium salts **47** in excellent yields and proved to be compatible with various  
 186 substitution patterns on both the (7-deaza)purine **46** as well as the alkyne **5**. Mechanistic studies  
 187 employing cyclic voltammetry demonstrated that the coordination of **46** to the Cp<sup>\*</sup>Rh(III) catalyst  
 188 and successive cyclometallation gives rhoda(III)-cycle **48**, which upon migratory insertion with  
 189 alkyne **5** and subsequent reductive elimination delivers the rhodium(I) sandwich complex **51**. By  
 190 anodic oxidation of complex **51** the annulated product **47** is released and the catalytically  
 191 competent rhodium(III) is regenerated (**Scheme 13**).<sup>[21]</sup>

192



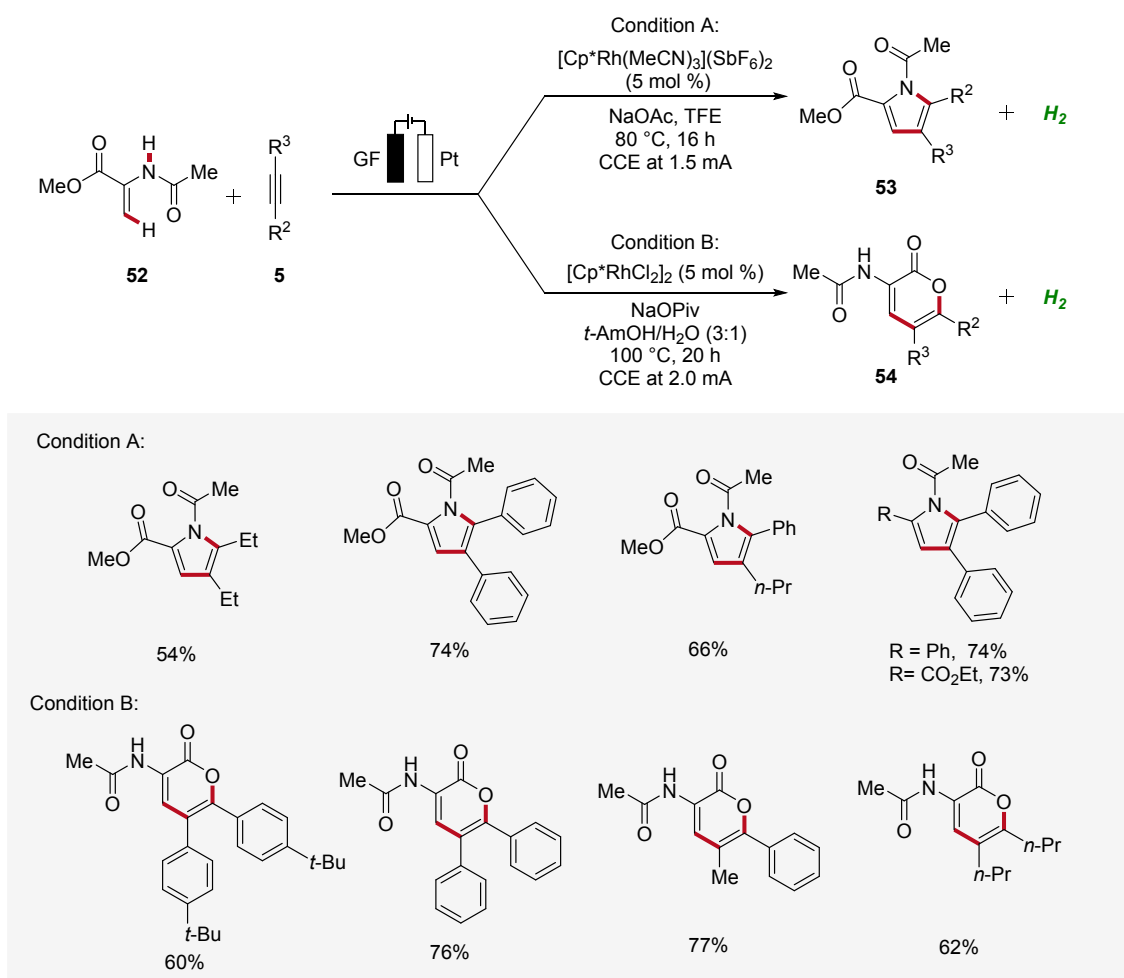




193

194 **Scheme 13:** Versatility and mechanism of rhodoelectro-catalyzed [4+2] C-H annulation.

195 Recently, Ackermann accomplished rhodaelectro-catalyzed C–H annulations using enamides **52**  
 196 and alkynes **5** in an user-friendly undivided cell setup (**Scheme 14**).<sup>[22]</sup> Interestingly, a bifurcated  
 197 reaction pathway was uncovered, where the solvent system was identified as crucial factor in  
 198 controlling the chemo-selectivity. Thus, through the rational choice of the reaction medium, the  
 199 product formation between pyrroles **53** and lactones **54** could be switched. This example  
 200 demonstrates how the ability to control chemo-selectivity broadens synthesis possibilities and  
 201 allows access to a wider range of heterocyclic structures.<sup>[22]</sup>



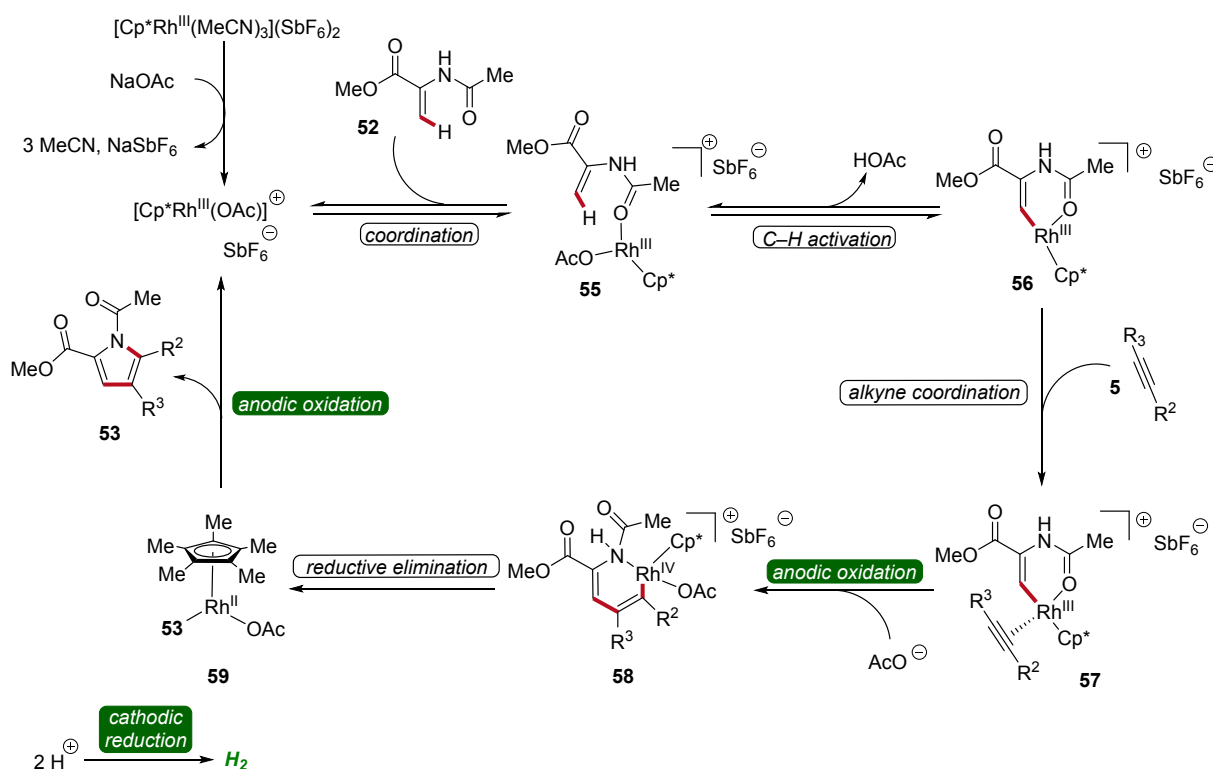
202

203 **Scheme 14:** Bifurcated rhodaelectro-catalyzed C–H annulation strategy for the synthesis of  
 204 pyrroles **53** and lactones **54**.

205 The bifurcated rhodaelectro-catalysis to construct pyrroles **53** or lactones **54** involves a multi-step  
 206 reaction mechanism (**Scheme 15**). Initially, the catalytically active Cp\*Rh(III) species is formed  
 207 followed by the coordination of enamide **52**, yielding intermediate **55**. Next, C–H activation takes



208 place to form rhoda(III)-cycle **56**. Thereafter, migratory insertion of alkyne **5** and anodic oxidation  
 209 results in the formation of rhodium(IV) species **58**, promoting a reductive elimination to form  
 210 intermediate **59**. The active rhodium(III) catalyst is then regenerated through anodic oxidation,  
 211 ultimately releasing product **53**. Regarding the chemo-divergence, it is proposed that the cathodic  
 212 hydrogen evolution reaction (HER) promotes the ester hydrolysis when an aqueous medium is  
 213 employed, initiating the divergent catalytic scenario primarily involving neutral rhodium  
 214 intermediates leading to lactones **54**.<sup>[22]</sup>



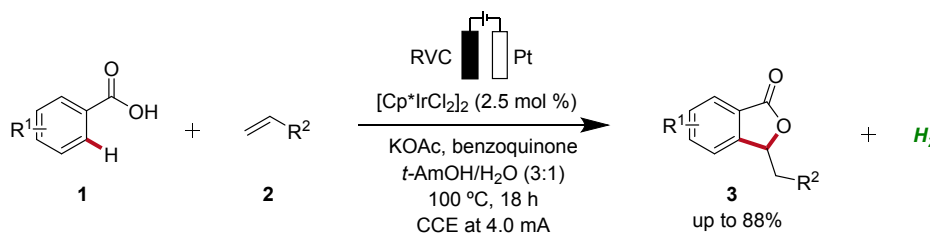
**Scheme 15:** Plausible catalytic cycle for the bifurcated rhodaelectro-catalyzed C–H annulation leading to pyrroles **53**.

218



219 **2.2 Iridaelectro-Catalyzed C–H Activation**

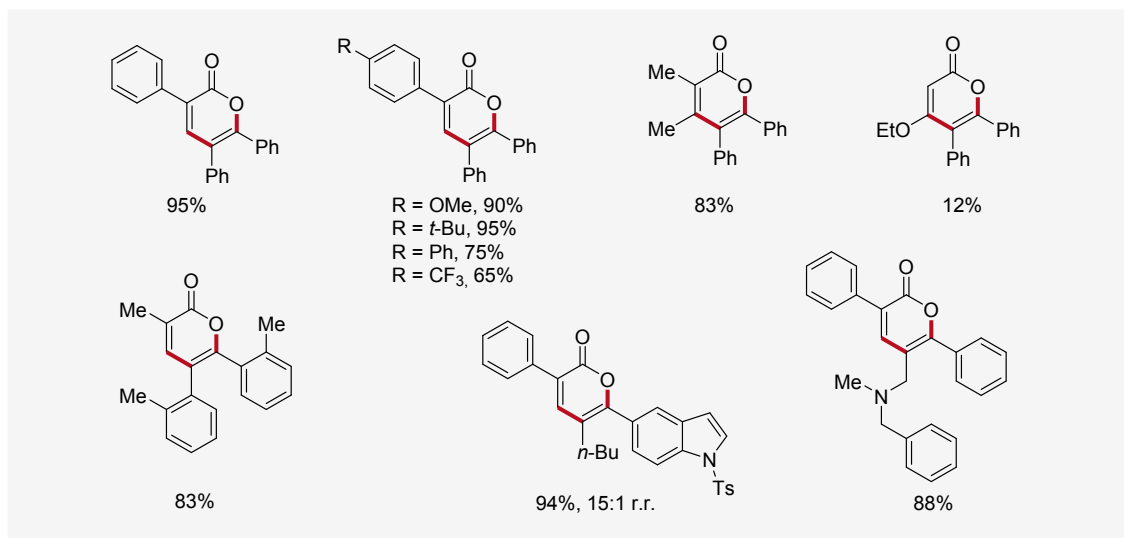
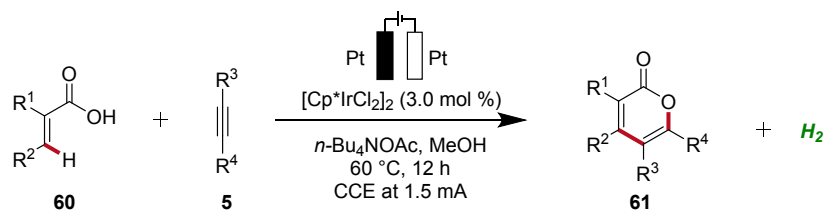
220 Iridium-catalyzed C–H activation has emerged as a powerful and versatile methodology in modern  
 221 organic synthesis.<sup>[23]</sup> In 2018, Ackermann developed the first irida-electrocatalyzed C–H  
 222 activation, which provided access to various isobenzofuranones **3** from benzoic acids **1** (**Scheme**  
 223 **16**).<sup>[24]</sup> With benzoquinone as redox catalyst an indirect, cooperative electrocatalysis was  
 224 uncovered.



226 **Scheme 16:** First iridaelectro-catalyzed C–H activation enabled by cooperative action of  
 227 benzoquinone as redox catalyst.

228 Thereafter, in 2019, Mei developed an irida-electrocatalyzed C–H annulation of acrylic acids **60**  
 229 to obtain biorelevant  $\alpha$ -pyrones **61** (**Scheme 17**).<sup>[25]</sup> The reaction conditions comprised  
 230 galvanostatic electrolysis in the presence of a  $[\text{Cp}^*\text{IrCl}_2]_2$  pre-catalyst. Various  $\alpha$ -substituted  
 231 acrylic acids **60** and internal alkynes **5** were tolerated, resulting in good to excellent yields of the  
 232 desired  $\alpha$ -pyrones **61**. The electrocatalysis demonstrated moderate to excellent regioselectivity  
 233 with unsymmetrical alkynes **5**.<sup>[25]</sup>



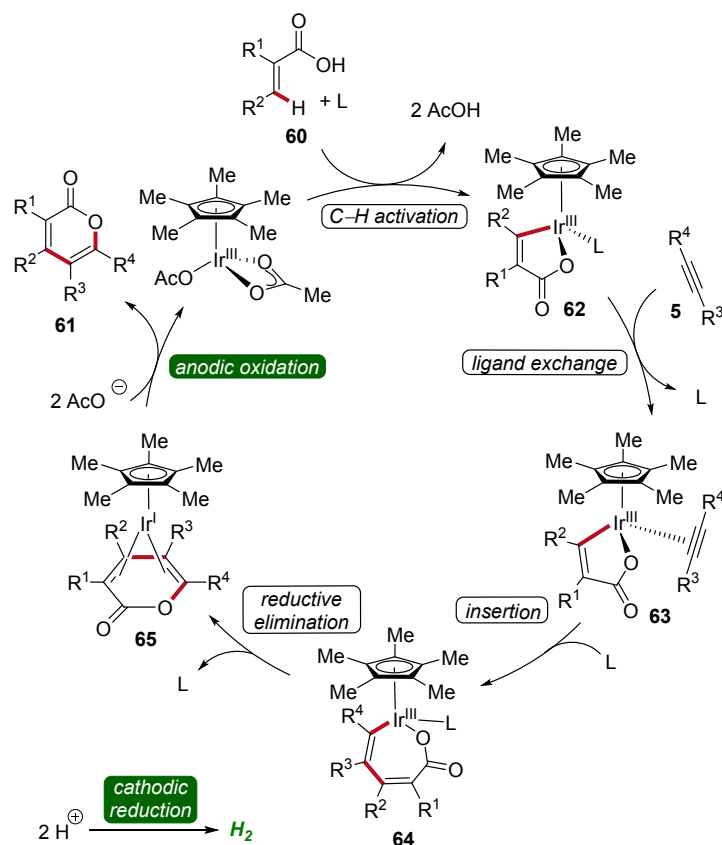


234

235 **Scheme 17:** Electrochemical iridium-catalyzed vinylic C–H annulation of acrylic acids **60**.

236 The irida-electrocatalysis proceeds in an Ir(III/I) regime (**Scheme 18**). The irida(III)-cycle **62** is  
 237 formed through carboxylate-assisted C–H activation, followed by coordination and insertion of  
 238 the alkyne **5**. Subsequently, by reductive elimination the sandwich complex **65** is formed, which,  
 239 through anodic oxidation, releases the product **61**.<sup>[25]</sup>



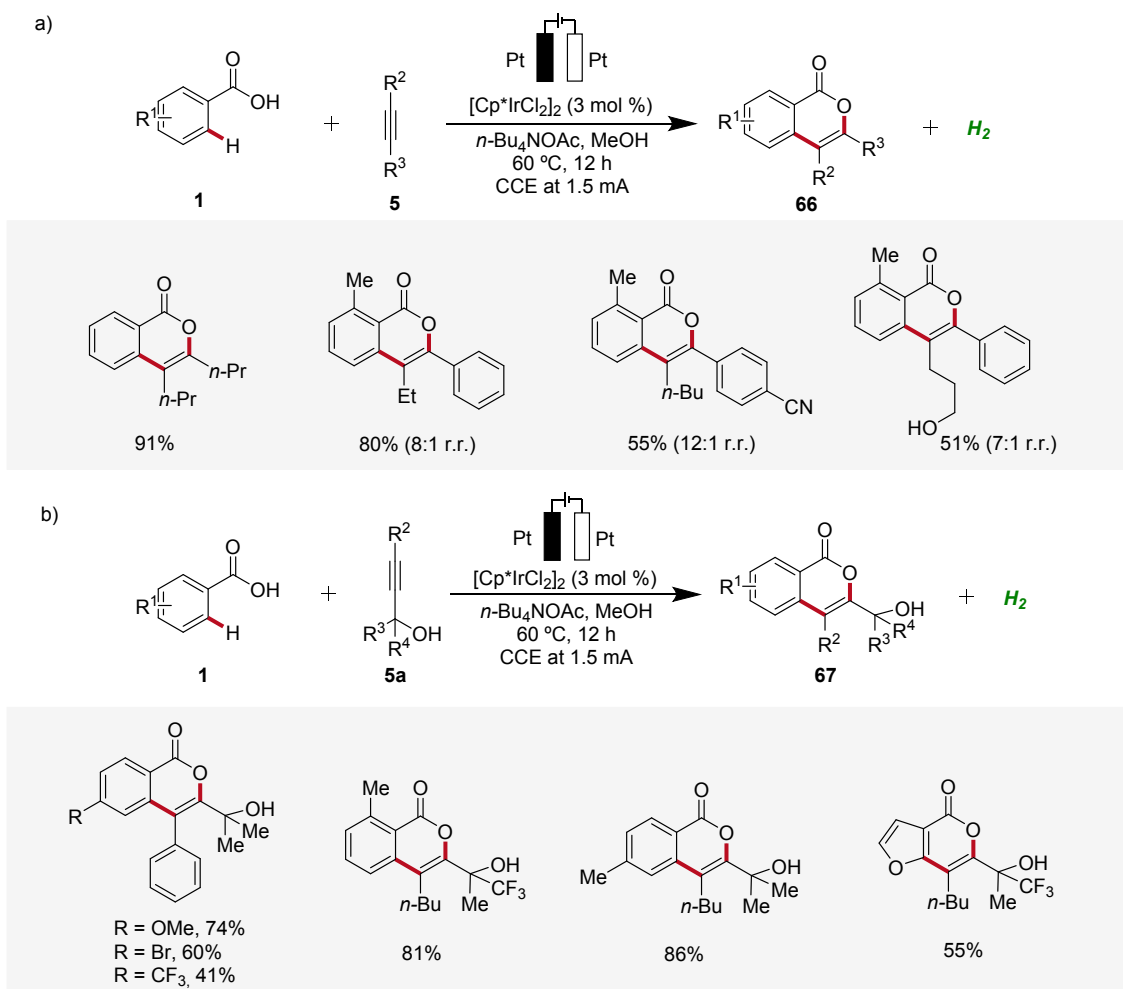


240

241 **Scheme 18:** Mechanism of iridium-catalyzed electrochemical vinylic C–H annulation of acrylic  
 242 acids **61**.

243 Isocoumarins are known for their significant biological effects and commonly found in natural  
 244 substances and medicinal compounds.<sup>[26]</sup> In 2021, Guo and Mei developed an iridoelectro-  
 245 catalyzed regioselective annulation of easily accessible aromatic carboxylic acids **1** with internal  
 246 alkynes **5** to access isocoumarins **66** with moderate to excellent regioselectivity (**Scheme 19**).<sup>[27]</sup>  
 247 The electrocatalysis demonstrated broad compatibility with various substrates **1** and **5**, including  
 248 dialkyl acetylenes. Mono-substituted benzoic acids **1** with electron-donating and electron-neutral  
 249 substituents readily reacted in satisfactory yields, while strong electron-withdrawing groups  
 250 afforded lower yields. However, with more sterically hindered arylalkynes the efficiency is  
 251 decreased (**Scheme 19a**). Interestingly, the reaction with *tert*-propargyl alcohols **5a** efficiently  
 252 furnished isocoumarins **67** under identical reaction conditions as a single regioisomer (**Scheme**  
 253 **19b**).<sup>[27]</sup>



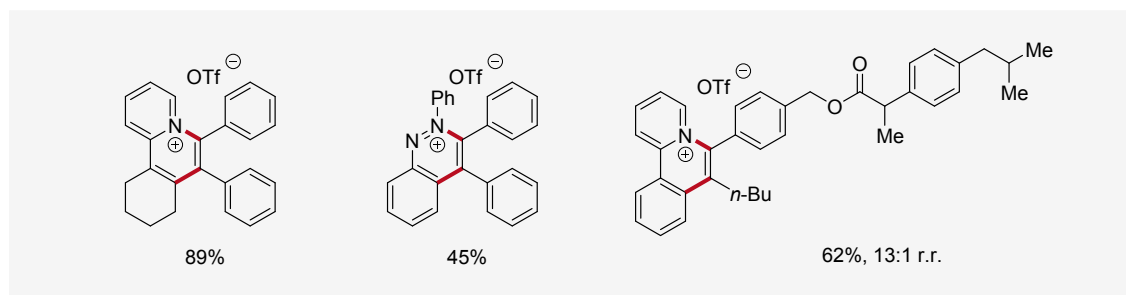
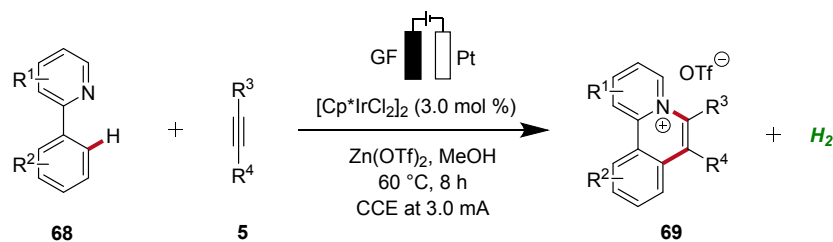


254

255 **Scheme 19:** Synthesis of isocoumarin derivatives **66** and **67** through irida-electrocatalysis.

256 Recently, Guo and Yang described an irida-electrocatalyzed C–H annulation, yielding cationic  $\pi$ -  
 257 extended heteroarenes **69** (Scheme 20).<sup>[28]</sup> The strategy demonstrated a broad substrate scope and  
 258 was compatible with various *N*-heteroarenes as directing groups, including pyridine and purine  
 259 derivatives. Additionally, mechanistic studies indicated an Ir(III/I) regime.<sup>[28]</sup>





**Scheme 20:** Synthesis of cationic  $\pi$ -extended heteroarenes **69** through irida-electrocatalysis.

260

261

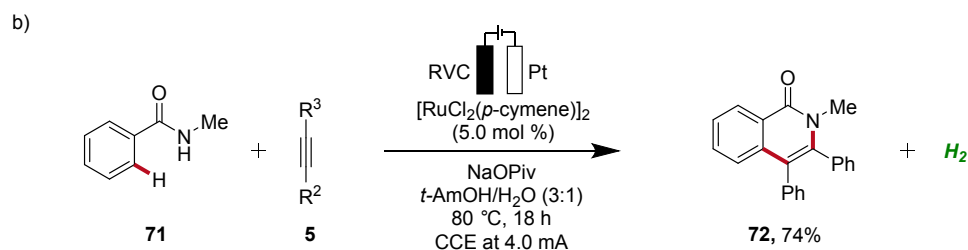
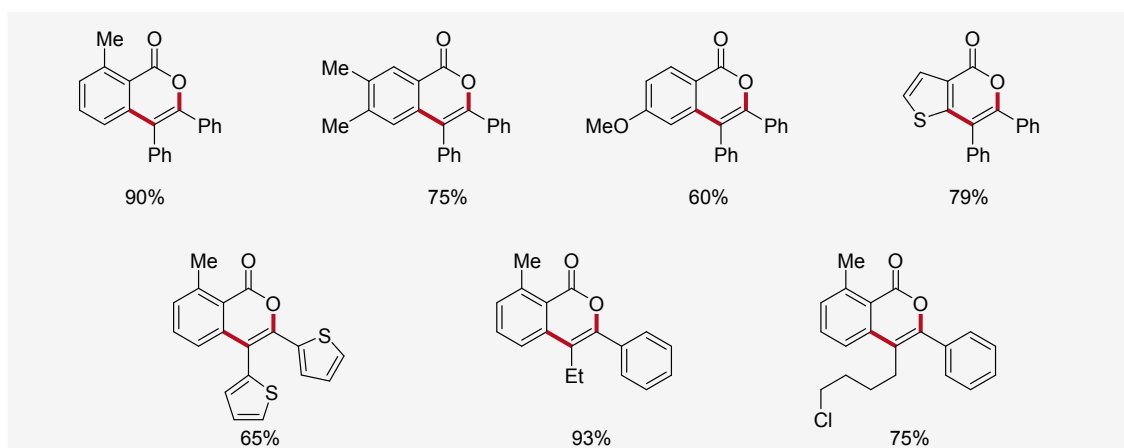
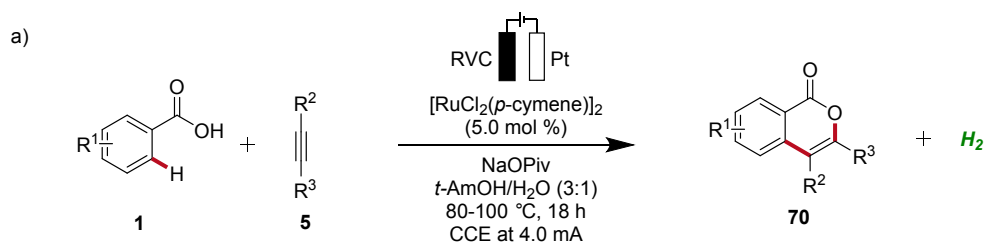
262





263 **2.3 Ruthenaelectro-Catalyzed C–H Activation**

264 Ruthenium catalysis is highly attractive due to the exceptional catalytic reactivity of ruthenium,  
 265 combined with its good availability compared to more expensive transition metals like palladium  
 266 and rhodium.<sup>[29]</sup> In 2018, Ackermann reported the first example of ruthenaelectro-catalyzed C–H  
 267 activation by weak *O*-coordination for the construction of isocoumarins **70** (Scheme 21).<sup>[30]</sup> The  
 268 reaction involves an *in situ* formed ruthenium(II) carboxylate catalyst mediating the C–H bond  
 269 activation in a reaction medium of *tert*-amyl alcohol and water. This ruthena-electrocatalysis  
 270 proved to be versatile and was amenable to both electron-rich as well as electron-deficient arenes  
 271 **1** and alkynes **5**. Notably, unsymmetrical alkynes **5** reacted to the desired product **70** with high  
 272 levels of regioselectivity (Scheme 21a). Additionally, the electrocatalysis was also found to be  
 273 compatible with benzamides **71**, to form the corresponding isoquinolones **72** (Scheme 21b).<sup>[30]</sup>

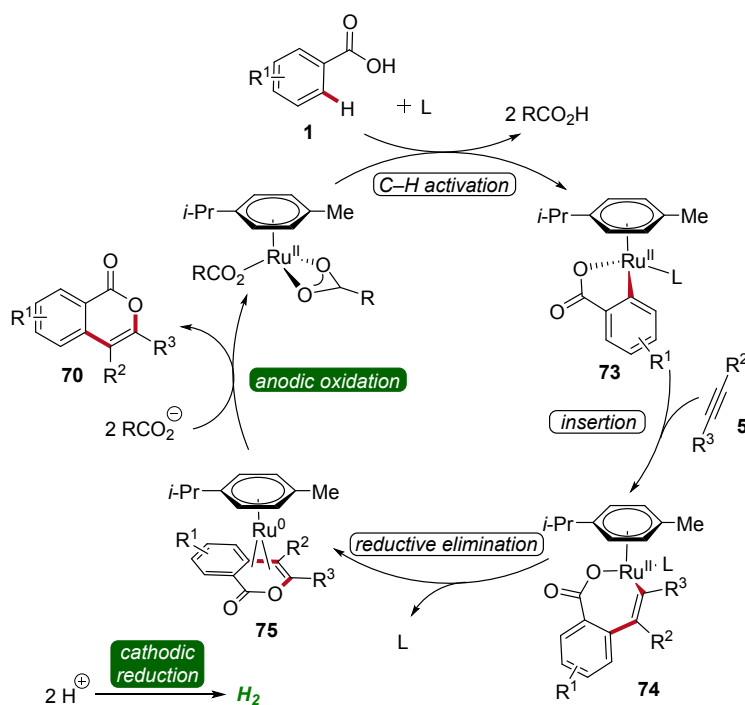


274



275 **Scheme 21:** Electro-oxidative ruthenium-catalyzed alkyne annulation to construct a) isocoumarins  
276 **70** and b) isoquinolones **72**.

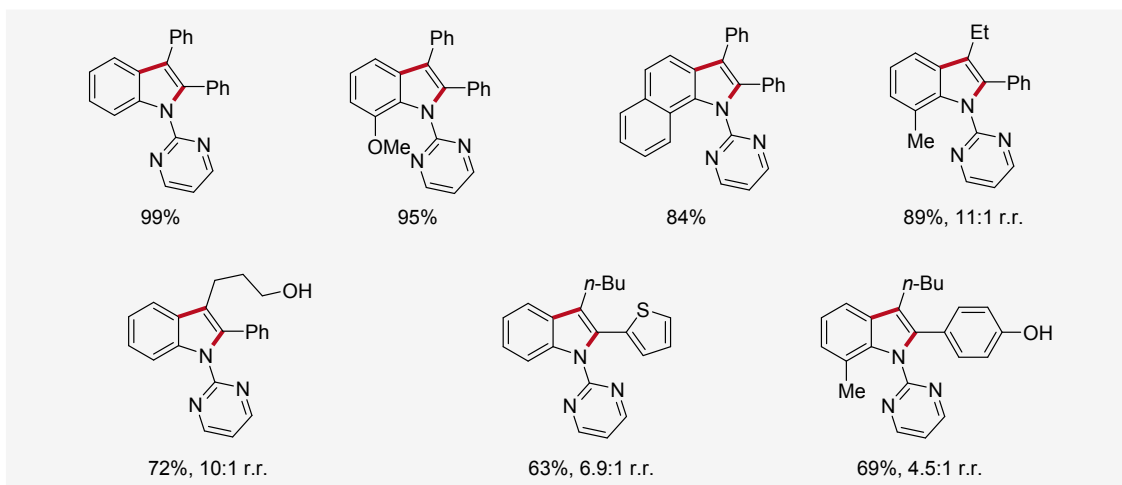
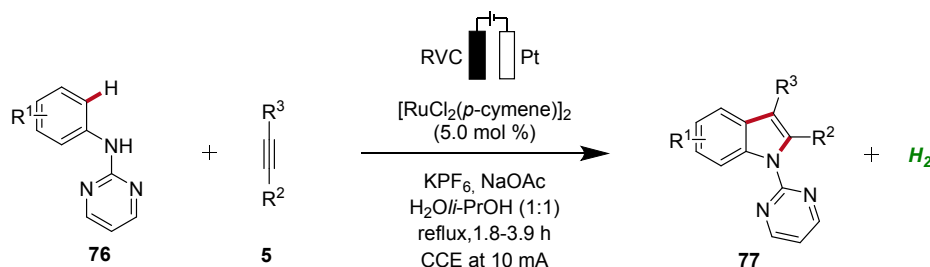
277 Based on detailed mechanistic studies, a plausible catalytic cycle was proposed (**Scheme 22**).  
278 Initially, the *ortho* C–H activation occurs, leading to the formation of the ruthena(II)-cycle **73**.  
279 Subsequently, the insertion of alkyne **5** takes place, forming the seven-membered ruthena(II)-cycle  
280 **74**, which undergoes reductive elimination to produce the ruthenium(0) sandwich complex **75**.  
281 This complex is then anodically oxidized, releasing product **70** and regenerating the catalytically  
282 competent ruthenium(II) carboxylate species, while cathodic reduction generates molecular  
283 hydrogen being the sole stoichiometric byproduct (**Scheme 22**).<sup>[30]</sup>



284  
285 **Scheme 22:** Catalytic cycle for the electro-oxidative ruthenium-catalyzed alkyne annulation by  
286 weakly coordinating benzoic acids **1**.

287 Concurrently, Xu developed a ruthenaelectro-catalyzed C–H annulation of anilines **76** with  
288 alkynes **5** in an undivided cell under galvanostatic electrolysis (**Scheme 23**).<sup>[31]</sup> The  
289 electrocatalysis allowed access to indoles **77** with diverse functional groups in good to excellent  
290 yields. However, substrates with highly sterically hindered functional groups exhibited diminished  
291 regioselectivity and reactivity.<sup>[31]</sup>



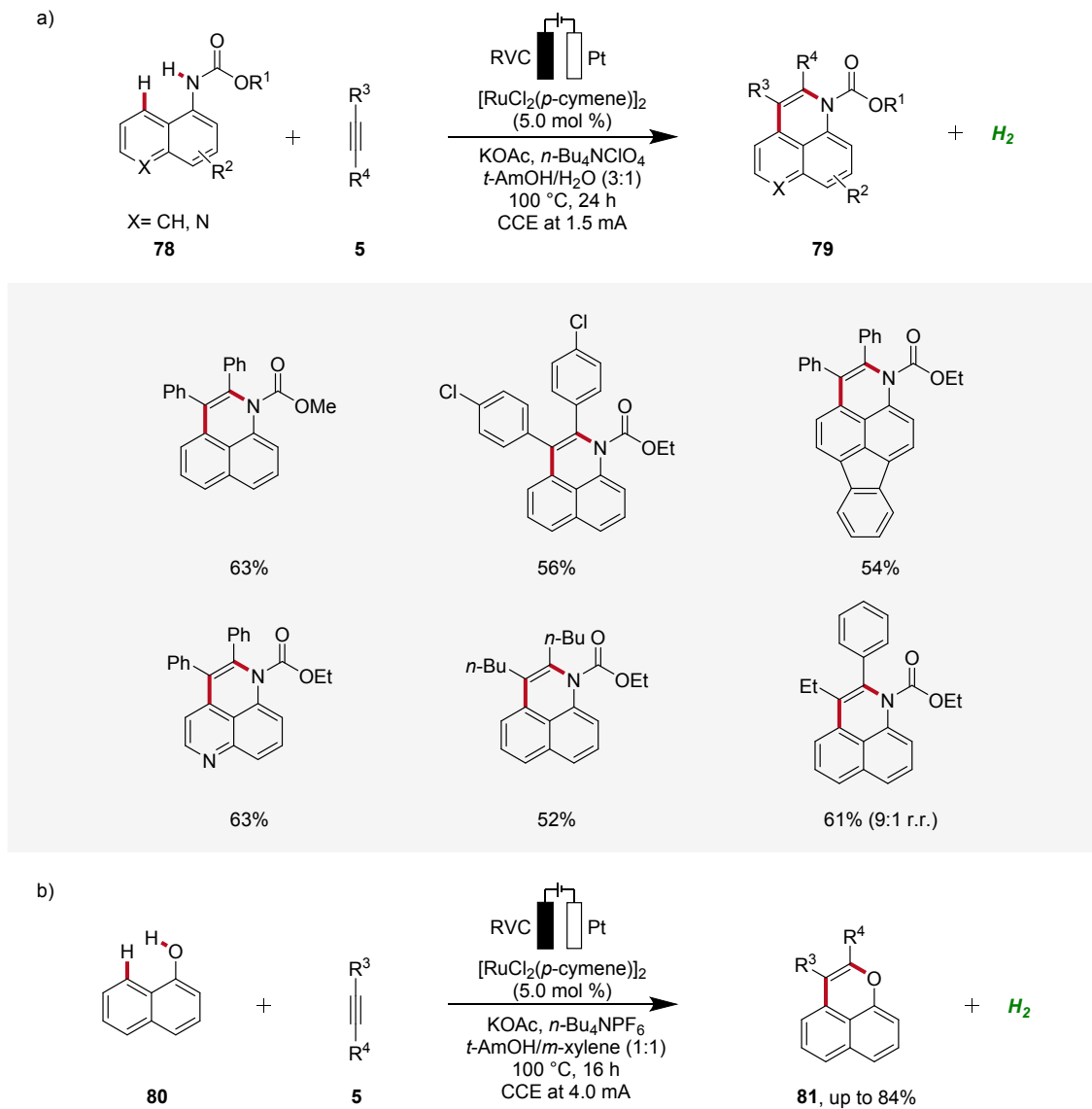


292

293 **Scheme 23:** Ruthenaelectro-catalyzed C–H/N–H annulation for the synthesis of indoles **77**.

294 In 2018, Ackermann established an electrochemical *peri*-selective C–H alkyne annulation of aryl  
 295 carbamates **78** and naphthols **80** using ruthenium-catalysis (**Scheme 24**).<sup>[32]</sup> Here, electrochemical  
 296 conditions for facilitating both C–H/N–H and C–H/O–H annulations were identified. The  
 297 versatility of this approach was assessed by varying the functional groups on both substrates  
 298 demonstrating excellent site-, regio-, and chemo-selectivity. The strategy provided access to  
 299 diverse benzoquinoline derivatives **79** and pyrans **81** in a step-economical manner with high  
 300 efficacy and selectivity.<sup>[32]</sup>

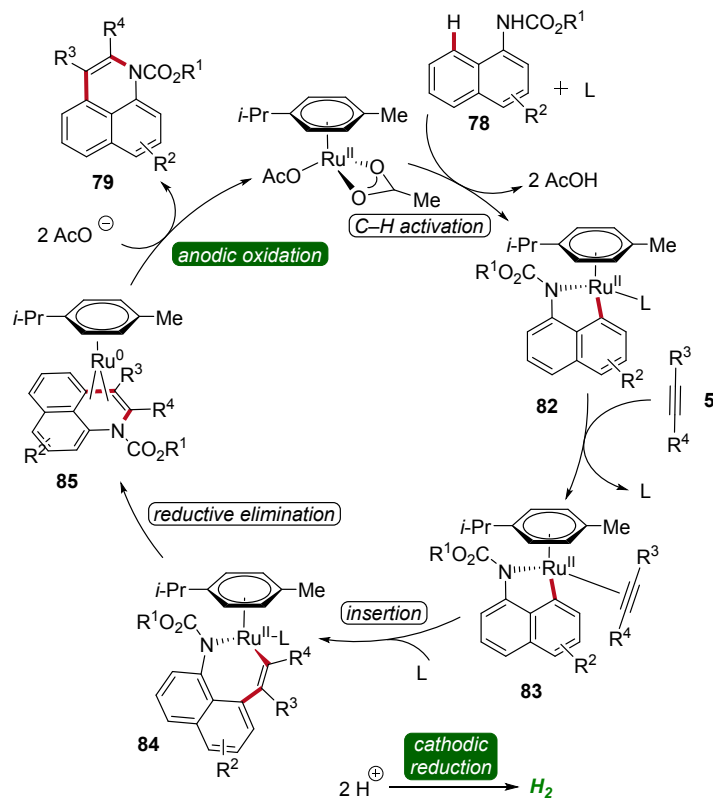




302 **Scheme 24:** Ruthenaelectro-catalyzed *peri*-selective C–H alkyne annulations to access  
303 benzoquinolines **79** and pyrans **81**.

304 Based on detailed mechanistic studies, a possible catalytic cycle was proposed (**Scheme 25**). The  
305 catalytic cycle begins with organometallic C–H activation, generating a ruthena(II)-cycle **82**.  
306 Migratory alkyne insertion then forms a seven-membered ruthena(II)-cycle **84**, which undergoes  
307 reductive elimination to produce a ruthenium(0)-sandwich complex **85**. The anodic oxidation of  
308 complex **88** results in the desired product **79**.<sup>[32]</sup>



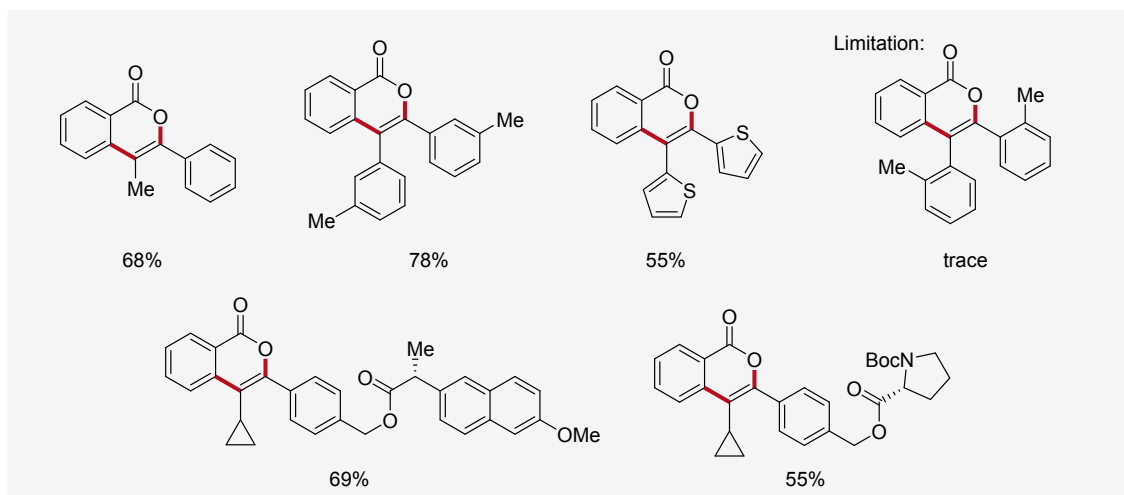
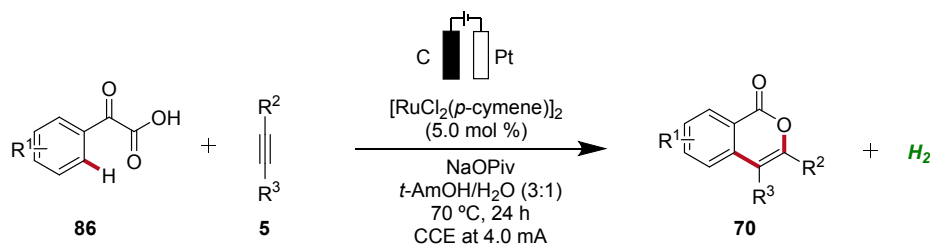


309

310 **Scheme 25:** Catalytic cycle for the ruthenaelectro-catalyzed alkyne annulation of arylcarbamates  
311 **78.**

312 In 2019, Li likewise employed ruthenaelectro-catalysis to access isocoumarins **70** (Scheme 26).<sup>[33]</sup>  
313 Here, an electrochemical decarboxylative C–H annulation strategy involving arylglyoxylic acids  
314 **86** and internal alkynes **5** was devised for the construction of isocoumarins **70**. This regime was  
315 applicable with both symmetrical and unsymmetrical internal alkynes **5** showing high levels of  
316 regioselectivity. However, sterically congested alkynes **5** as well as electron-withdrawing  
317 functional groups on the arylglyoxylic acid **86** resulted in low efficiency of the electrocatalysis.<sup>[33]</sup>



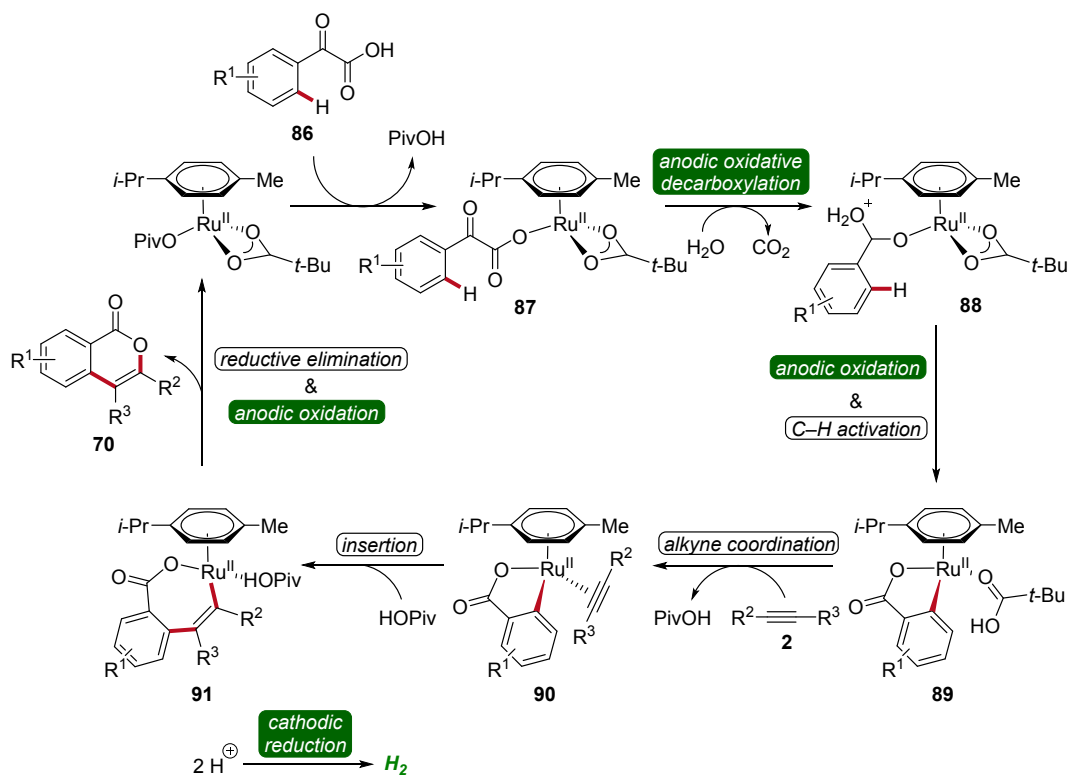


318

319 **Scheme 26:** Decarboxylative ruthena-electro-catalyzed C–H annulation to access isocoumarins **70**.

320 To gain mechanistic insights of the decarboxylative ruthena-electrocatalysis, <sup>18</sup>O-labeled isotope  
 321 and kinetic isotope effect experiments were conducted. Here, a cooperative action of the anodic  
 322 decarboxylation and C–H activation was found. The reaction initiates with the carboxyl group of  
 323 the arylglyoxylic acid **86** coordinating to the active ruthenium(II) carboxylate species, leading to  
 324 the formation of intermediate **87**. Subsequently, this intermediate undergoes anodic single-electron  
 325 oxidation to promote a decarboxylation and hydration to yield intermediate **88**. Next, further  
 326 anodic oxidation along with C–H activation leads to ruthena(II)-cycle **89** and the migratory  
 327 insertion of alkyne **5** to generate the seven-membered ruthena(II)-cycle **91** is realized. Lastly,  
 328 reductive elimination takes place, resulting in the formation of desired product **70** and the active  
 329 ruthenium(II) carboxylate species is regenerated by anodic oxidation (**Scheme 27**).<sup>[33]</sup>

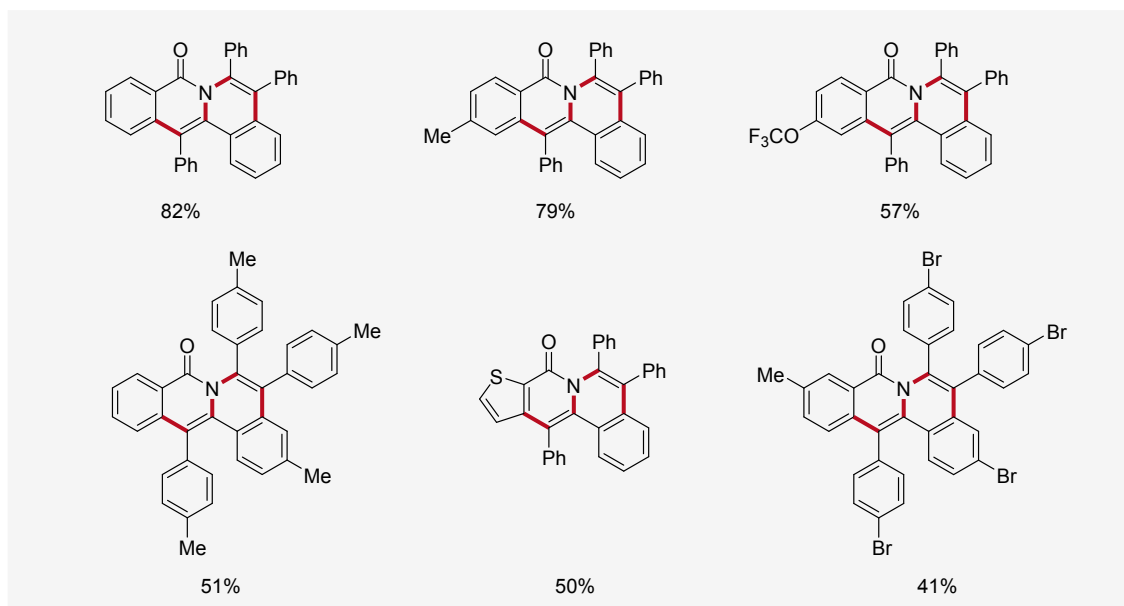
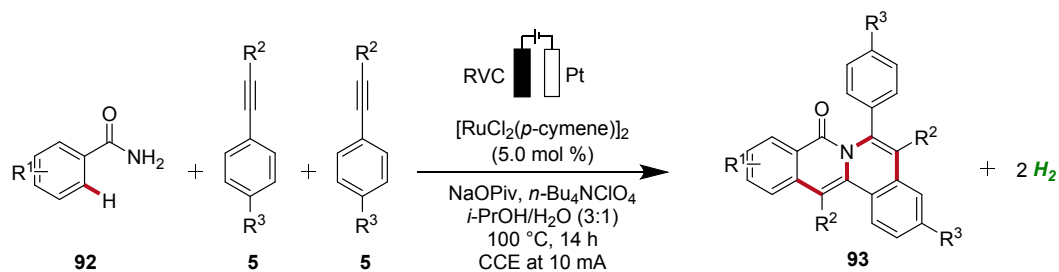




**Scheme 27:** Mechanism of the decarboxylative ruthenalectro-catalyzed C–H annulation.

In 2019, Tang developed an electrocatalytic method for synthesizing polycyclic isoquinolinones **93** through double C–H activation (**Scheme 28**).<sup>[34]</sup> The reaction was effective using a simple undivided cell under galvanostatic electrolysis and was compatible with a wide range of benzamides **92** and alkynes **5** yielding the desired fused products **93** with medium to excellent yields. The high site-selectivity of the electrocatalysis was further demonstrated by using *meta*-substituted benzamides **92**.<sup>[34]</sup>





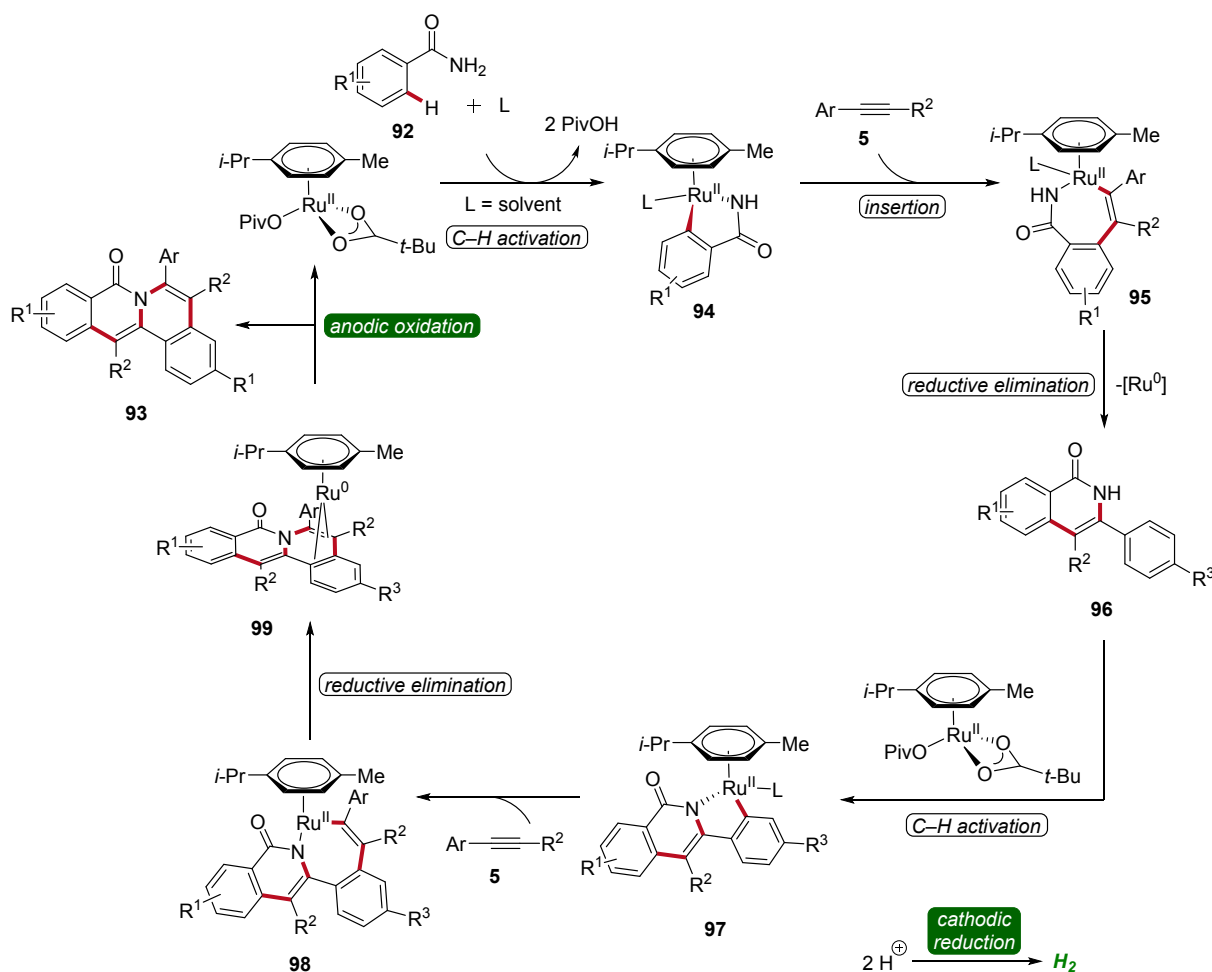
338

339 **Scheme 28:** Ruthenaelectro-catalyzed C–H annulation for the chemoselective synthesis of  
 340 polycyclic isoquinolinones **93**.

341 The initial step of the proposed mechanism involves the formation of ruthena(II)-cycle **94** through  
 342 C–H activation. Subsequently, the insertion of alkyne **5** leads to intermediate **95**, which then  
 343 undergoes reductive elimination to furnish **96**. This is followed by a second C–H activation event,  
 344 resulting in the formation of yet another cyclometallated intermediate **97**. Through a sequence  
 345 involving the insertion of a second alkyne **5** and subsequent reductive elimination, the  
 346 ruthenium(0) sandwich complex **99** is formed. Ultimately, product **93** is released from complex  
 347 **99** through anodic oxidation (**Scheme 29**).<sup>[34]</sup>



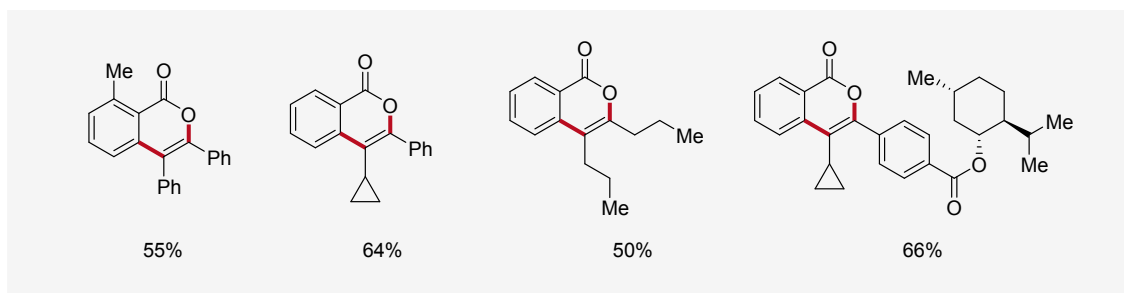
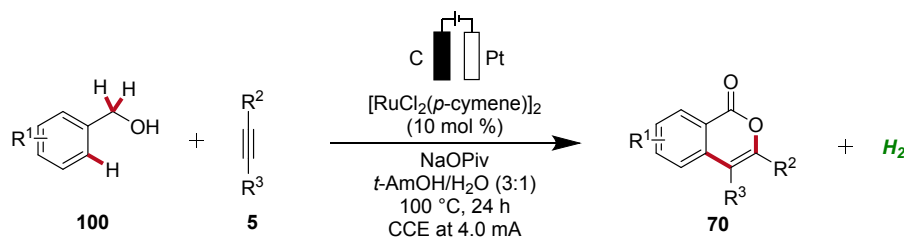




**Scheme 29:** Simplified catalytic cycle for the ruthenaelectro-catalyzed double C–H activation.

Li applied the ruthenaelectro-catalyzed C–H annulation strategy for the synthesis of isocoumarin cores **70** from primary benzylic alcohols **100** (Scheme 30).<sup>[35]</sup> Notably, this regime allowed benzylic alcohols **100** to act as weakly directing group precursors to acquire isocoumarins **70** via multiple C–H functionalizations. The electrocatalysis displayed high regio- and site-selectivity with a broad substrate scope. In contrast to internal alkynes **5**, terminal alkynes were not found to be compatible with this strategy.<sup>[35]</sup>

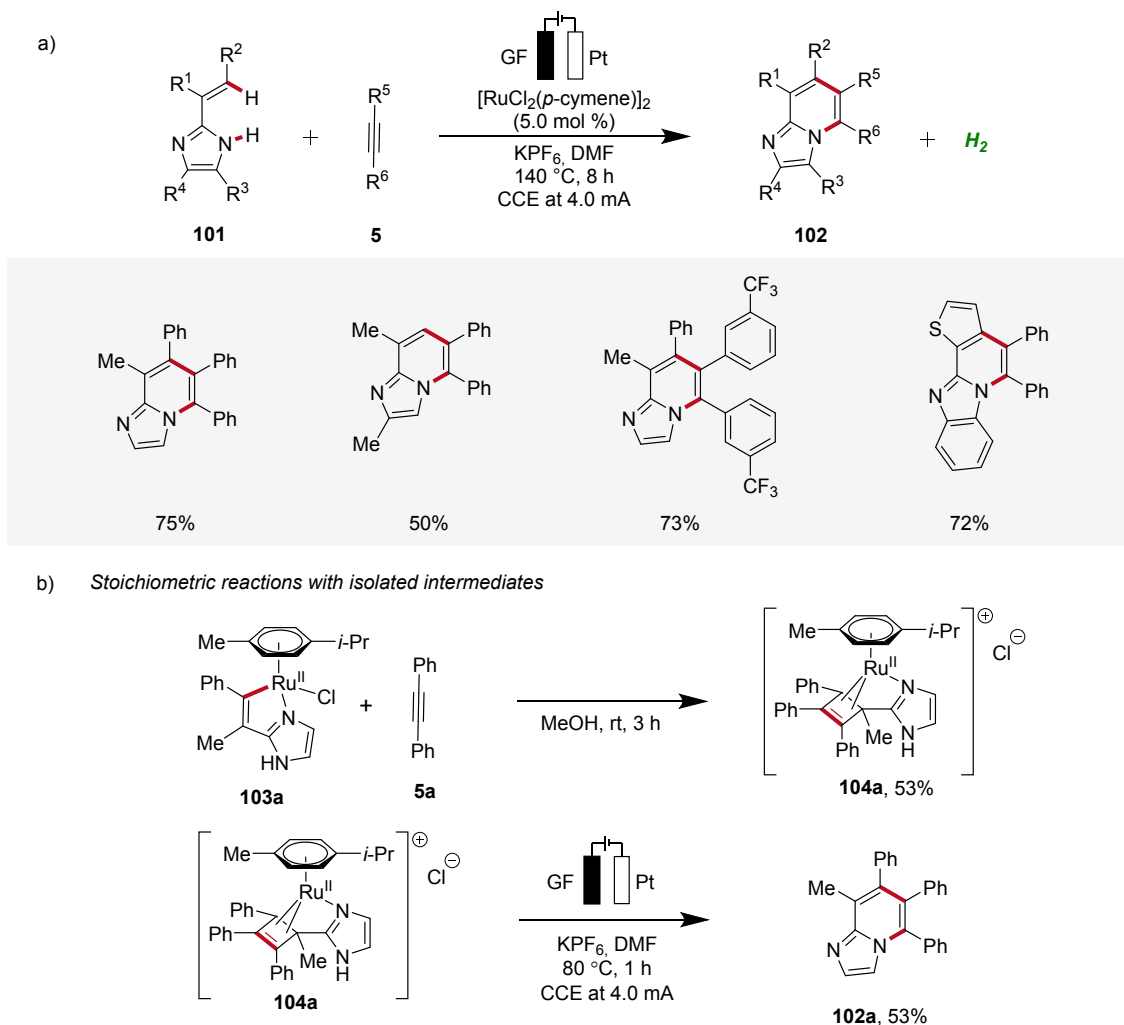




356  
357 **Scheme 30:** Ruthenaelectro-catalyzed C–H annulations for the synthesis of isocoumarins **70** from  
358 benzylic alcohols **100**.

359 In 2020, Ackermann further demonstrated a ruthena-electrocatalysis for the assembly of diverse  
360 bridgehead *N*-fused [5,6]-bicyclic heteroarenes **102** from imidazoles **101** with alkynes **5**, involving  
361 an oxidation-induced reductive elimination pathway (**Scheme 31**).<sup>[36]</sup> The versatility of this  
362 strategy was explored with various imidazole **101** and alkyne **5** substrates decorated with a range  
363 of substituents at different positions, amenable to efficiently form the desired products **102**.  
364 Besides alkenyl imidazoles, also 2-arylimidazoles **101** were applicable (**Scheme 31a**). Notably,  
365 organometallic azaruthena(II)-bicyclo[3.2.0]heptadiene intermediates **103a** and **104a** were  
366 isolated and employed in stoichiometric reactions, providing strong support for an oxidation-  
367 induced reductive elimination within a ruthenium(II/III/I) manifold (**Scheme 31b**).<sup>[36]</sup>



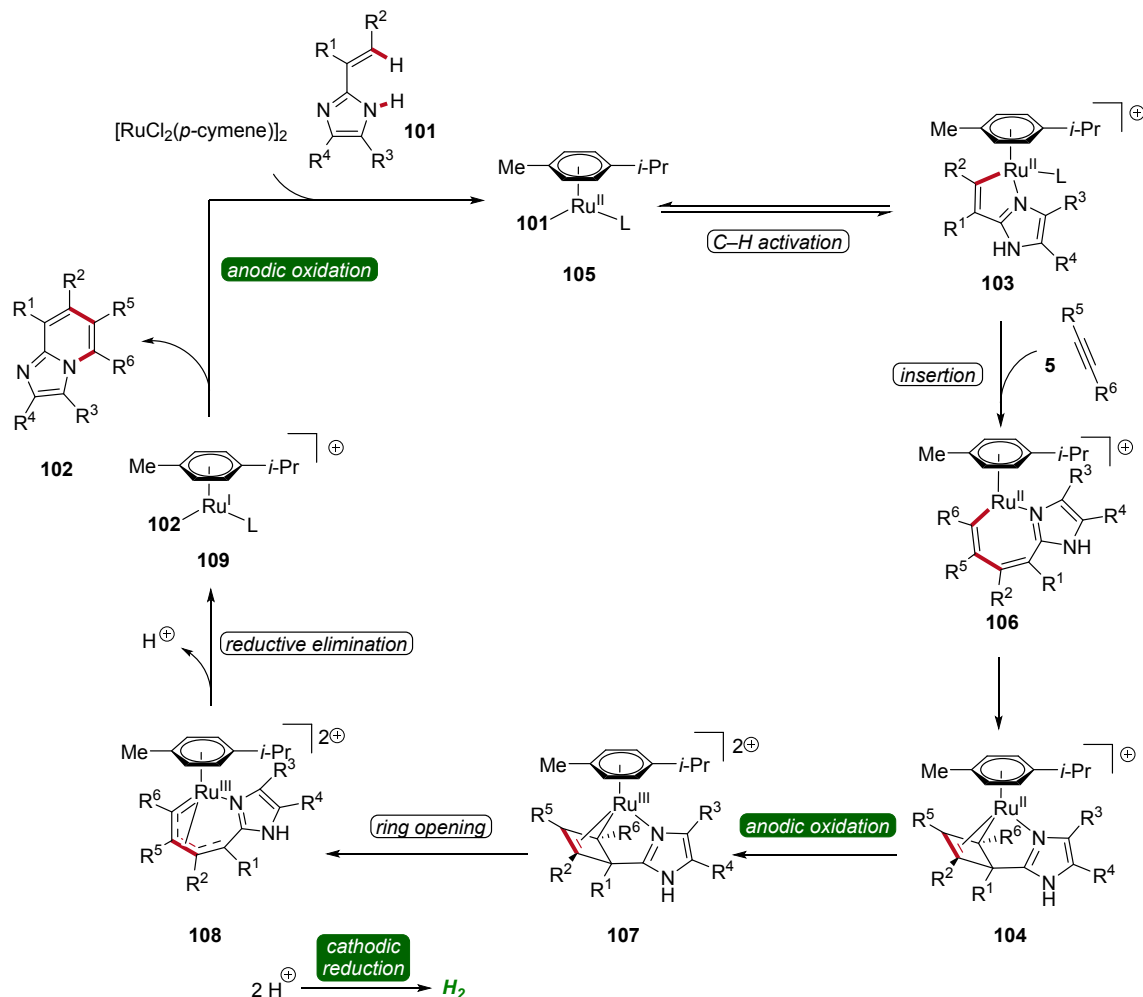


368

369 **Scheme 31:** Ruthenaelectro-catalyzed synthesis of bridgehead *N*-fused [5,6]-bicyclic heteroarenes  
370 **102.**

371 Hence, the azaruthena(II)-bicyclo[3.2.0]heptadiene intermediate **104** formed through alkyne  
372 coordination and migratory insertion to the ruthena(II)-cycle **103** undergoes anodic oxidation to  
373 form the ruthenium(III) complex **107**, followed by a pericyclic ring opening to yield **108**.  
374 Reductive elimination then yields the ruthenium(I) complex **109**, which releases the final *N*-fused  
375 [5,6]-bicyclic heteroarene **102** (Scheme 32).<sup>[36]</sup>

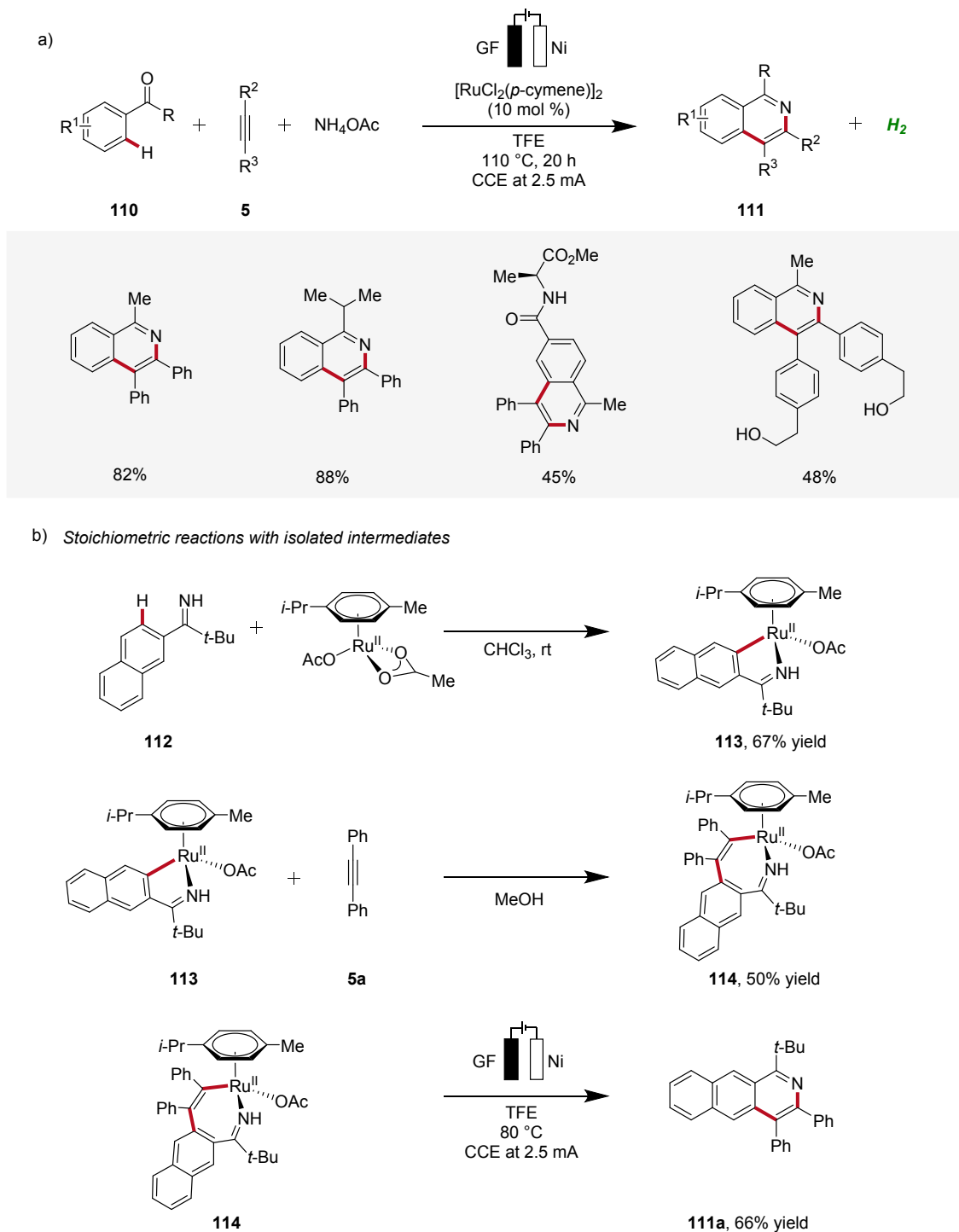




**Scheme 32:** Plausible catalytic cycle for the ruthenaelectro-catalyzed annulation involving azaruthena(II)-bicyclo[3.2.0]heptadiene intermediates.

379 In 2020, Ackermann reported on a ruthenaelectro-catalyzed domino three-component alkyne C–H  
 380 annulation, which enabled the expedient construction of isoquinolines **111** from phenones **110**,  
 381 alkynes **5**, and ammonium acetate (**Scheme 33**).<sup>[37]</sup> The reaction demonstrated a broad substrate  
 382 scope, including the compatibility with unprotected alcohol groups. Additionally, relevant  
 383 cyclometallated ruthenium species **113** and **114** were isolated and their significance for the  
 384 electrocatalysis was evaluated, supporting a ruthenium(II/III/I) pathway.<sup>[37]</sup>



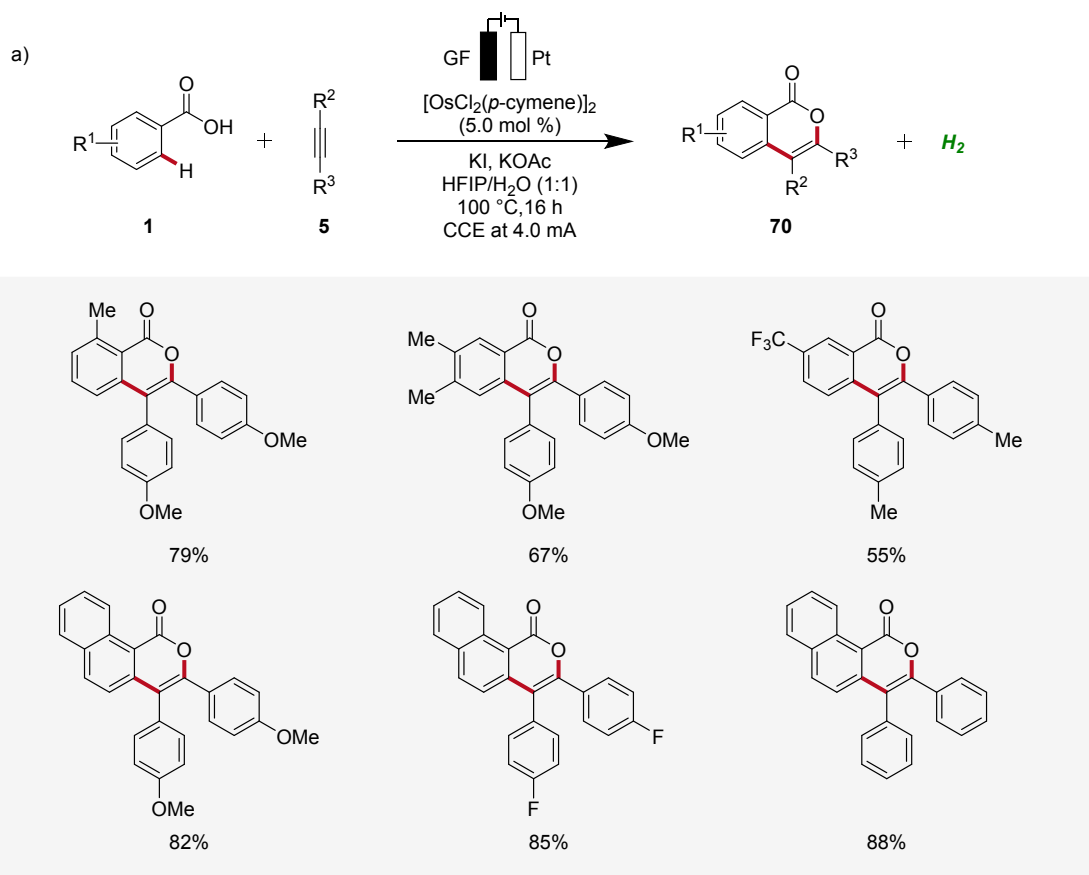
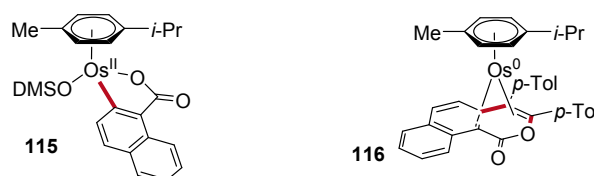


385

386 **Scheme 33:** Domino three-component alkyne C–H annulation enabled by ruthena-electrocatalysis.

387 **2.4 Osmaelectro-Catalyzed C–H Activation**

388 Osmium, a transition-metal known for its robust reactivity and versatile coordination chemistry,  
 389 serves as a remarkable catalyst in various redox processes.<sup>[38]</sup> In 2021, Ackermann described the  
 390 first osmaelectro-catalyzed C–H activation (**Scheme 34a**).<sup>[39]</sup> The strategy allowed expedient  
 391 access to isocoumarins **70** from benzoic acids **1** and alkynes **5** with a broad tolerance to functional  
 392 groups. Furthermore, systematic reaction monitoring by NMR spectroscopy and HR-ESI-mass  
 393 spectrometry provided support for an osmium(II/0) manifold, while key organometallic  
 394 intermediates **115** and **116** were isolated and studied (**Scheme 34b**).<sup>[39]</sup>

b) *Isolated intermediates*

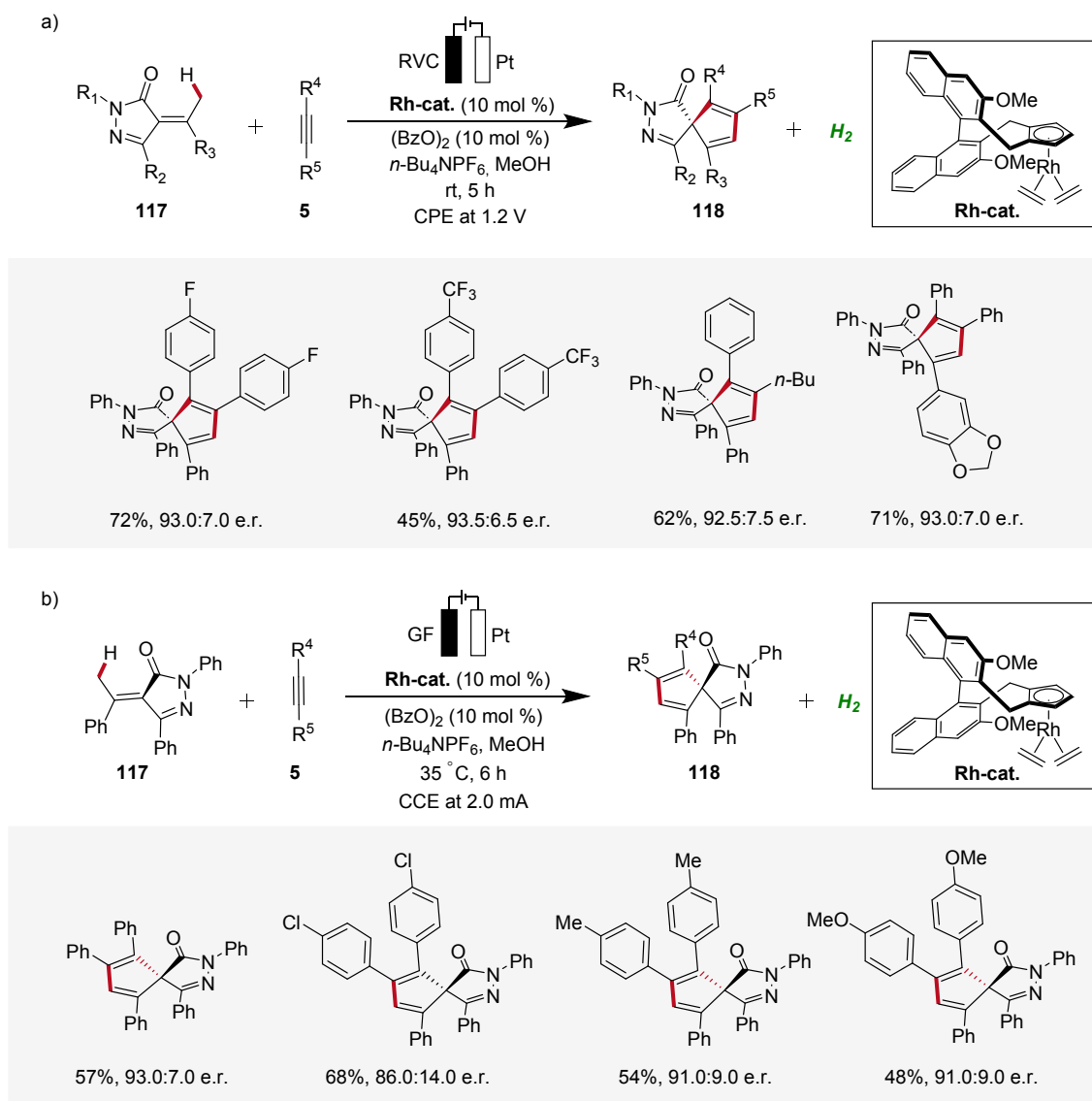
395

396 **Scheme 34:** Osmaelectro-catalyzed alkyne annulation by weakly coordinating acids **1**.

## 397 2.5 Enantioselective 4d Metallalectro-Catalyzed Alkyne Annulations

398 In recent years, enantioselective electrocatalysis has emerged as an increasingly versatile tool for  
399 the assembly of complex molecules.<sup>[40]</sup> Pioneering work in the domain of enantioselective 4d-  
400 metallalectro-catalyzed C–H activation was contributed by Ackermann in 2020, where  
401 palladaelectro-catalyzed C–H alkenylations were disclosed to construct axially chiral biaryls.<sup>[41]</sup>  
402 Thereafter, in 2021, Mei reported on an enantioselective rhodaelectro-catalyzed C–H annulation  
403 for the synthesis of biorelevant spiropyrazolones **118** by reacting  $\alpha$ -arylidene pyrazolones **117** with  
404 alkynes **5** in an undivided cell under potentiostatic electrolysis (**Scheme 35a**).<sup>[42]</sup> This robust  
405 annulation strategy provided access to a variety of chiral spirocycles **118** in decent yields and  
406 enantioselectivities.<sup>[42]</sup> Concurrently, Ackermann established an enantioselective rhodaelectro-  
407 catalyzed strategy for the assembly of chiral spiropyrazolones **118**, operating under galvanostatic  
408 electrolysis (**Scheme 35b**). In this study, Ackermann also demonstrated a palladaelectro-catalyzed  
409 spiroannulation with alkynes, although without enantioselectivity.<sup>[43]</sup>



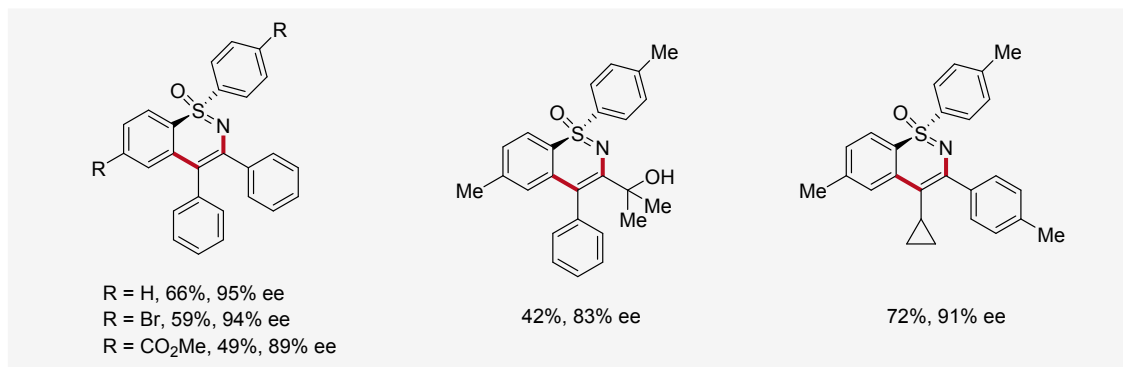
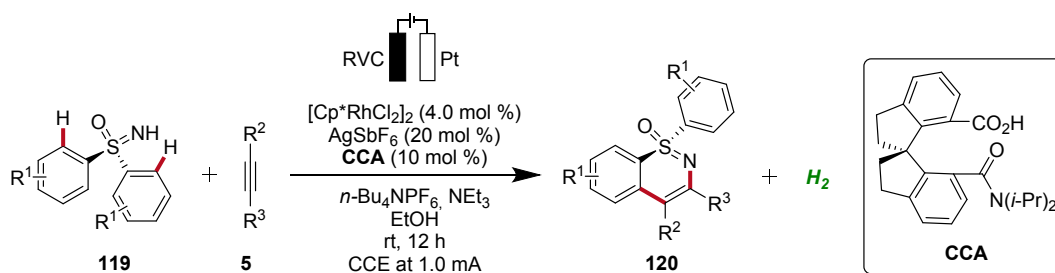


411 **Scheme 35:** Enantioselective rhodaelectro-catalyzed C–H annulations for the synthesis of  
412 spiropyrazolones **118**.

413 Very recently, Shi and Zhou applied the rhoda-electrocatalysis strategy<sup>[12]</sup> to the C–H annulation  
414 of sulfoximines **119**, where a chiral carboxylic acid (CCA) was effective in controlling  
415 enantioselectivity.<sup>[44]</sup> The *S*-stereogenic products **120** were obtained in moderate to good yields  
416 and enantioselectivities (**Scheme 36**).<sup>[44]</sup>







417

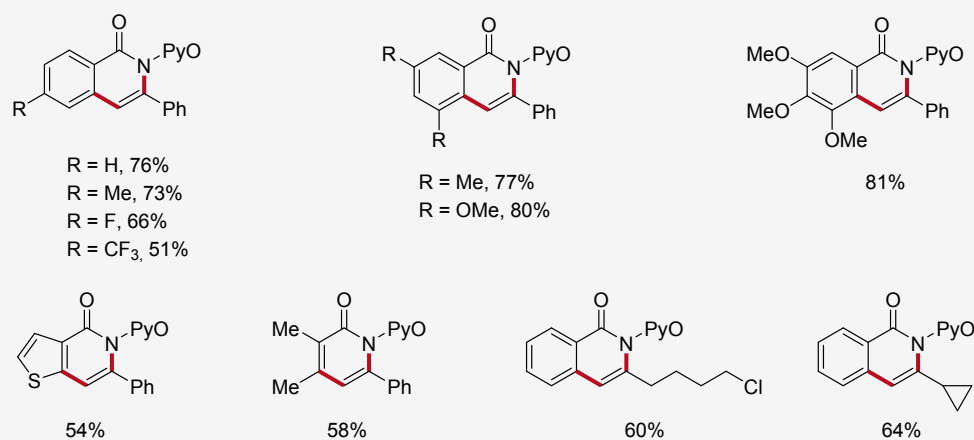
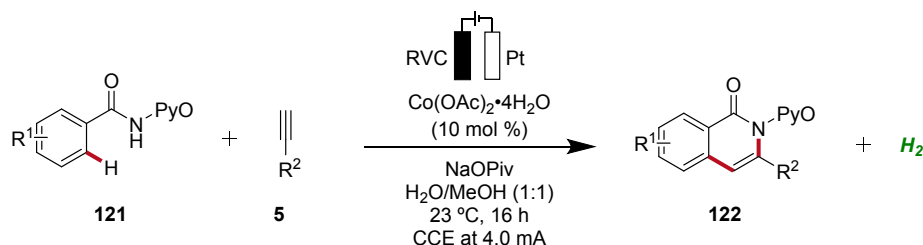
418 **Scheme 36:** Enantioselective rhodaelectro-catalyzed C–H annulation of sulfoximines **119**.

419



420 **3 3d Metallalectro-Catalyzed Alkyne Annulations**421 **3.1 Cobaltalelectro-Catalyzed C–H Activation**

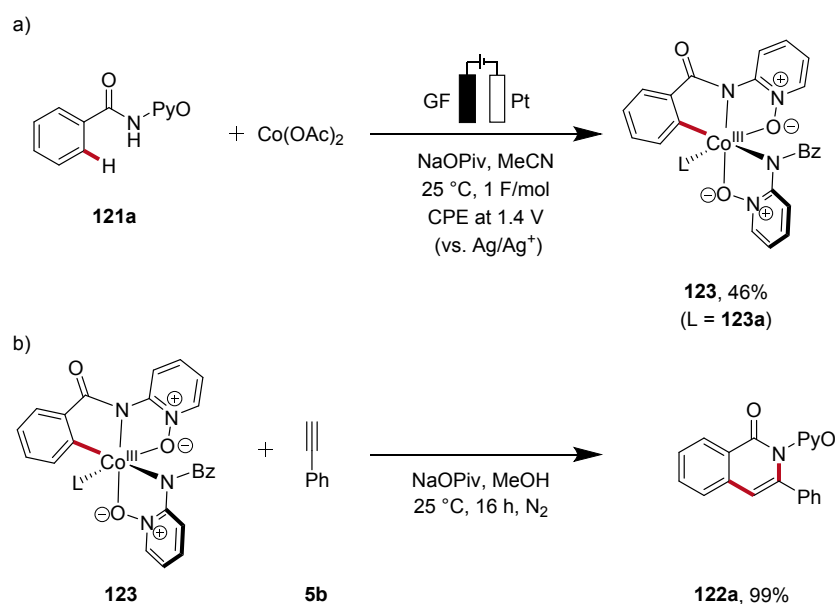
422 Cobalt, an economically viable and Earth-abundant transition metal, has emerged as one of the  
 423 foremost contenders for facilitating carbon–carbon and carbon-heteroatom bond-forming  
 424 reactions.<sup>[45]</sup> In 2018, Ackermann reported on the first cobaltalelectro-catalyzed C–H/N–H alkyne  
 425 annulation of benzamides **121** (Scheme 37).<sup>[46]</sup> The synthesis of isoquinolinones **122** was achieved  
 426 under exceedingly mild and environmentally-friendly conditions, employing an undivided cell  
 427 equipped with a platinum plate cathode and a reticulated vitreous carbon (RVC) anode under  
 428 galvanostatic electrolysis. In particular, the pyridine oxide directing group (PyO) proved to be  
 429 suitable for facilitating the electrocatalytic C–H/N–H annulation. Under the optimized  
 430 electrochemical conditions, a wide substrate scope was identified, demonstrating broad  
 431 applicability. Thus, alkynes **5** having cyclopropyl, alkyl chloride, and ester functional groups were  
 432 found to be viable substrates.<sup>[46]</sup>



433  
 434 **Scheme 37:** Cobaltalelectro-catalyzed C–H/N–H alkyne annulation with benzamides **121**.



435 Recently, in 2020, Ackermann reported key studies that provided mechanistic insights into the  
 436 mode of action of cobalta-electrocatalysis (**Scheme 38**).<sup>[47]</sup> Herein, the electrosynthesis of the  
 437 cyclometallated cobalt(III) complex **123** was achieved, which was further confirmed to be a key  
 438 intermediate in the electrocatalytic process (**Scheme 38a**). Thus, when this intermediate **123** is  
 439 reacted with the alkyne **5b** in the absence of electricity, the annulated product **122a** is formed in  
 440 99% yield (**Scheme 38b**). This result verifies a facile reductive elimination from cobalt(III) for the  
 441 C–H/N–H annulation without the need for an oxidation to cobalt(IV), as found for the C–O bond  
 442 forming pathway in C–H alkoxylation via oxidation-induced reductive elimination.<sup>[47]</sup>

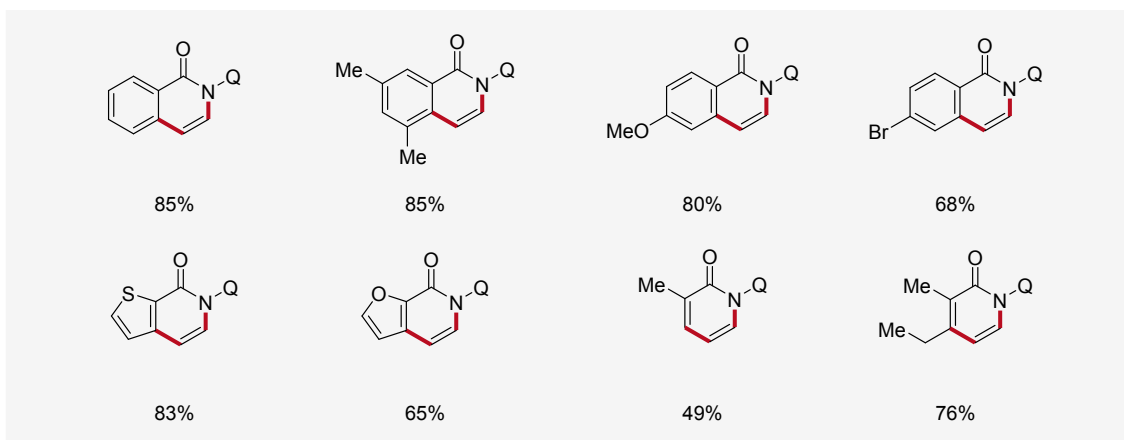
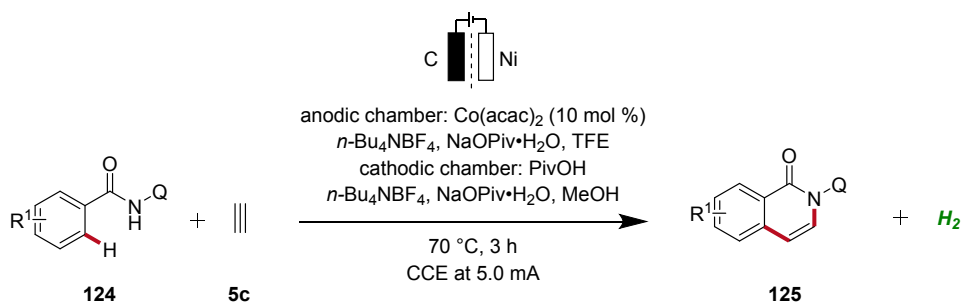


443

444 **Scheme 38:** Key experiments to unveil the mechanism of the C–H/N–H alkyne annulation.

445 Concurrently, Lei applied the cobalt electro-catalyzed C–H annulation strategy using 8-quinolinyl  
 446 (Q) substituted benzamides **124** and ethyne **5c** using a divided cell setup to yield isoquinolinones  
 447 **125** (**Scheme 39**).<sup>[48]</sup> This approach exhibited broad substrate scope, tolerating various benzamide  
 448 and acrylamide derivatives **124** as suitable substrates.<sup>[48]</sup>



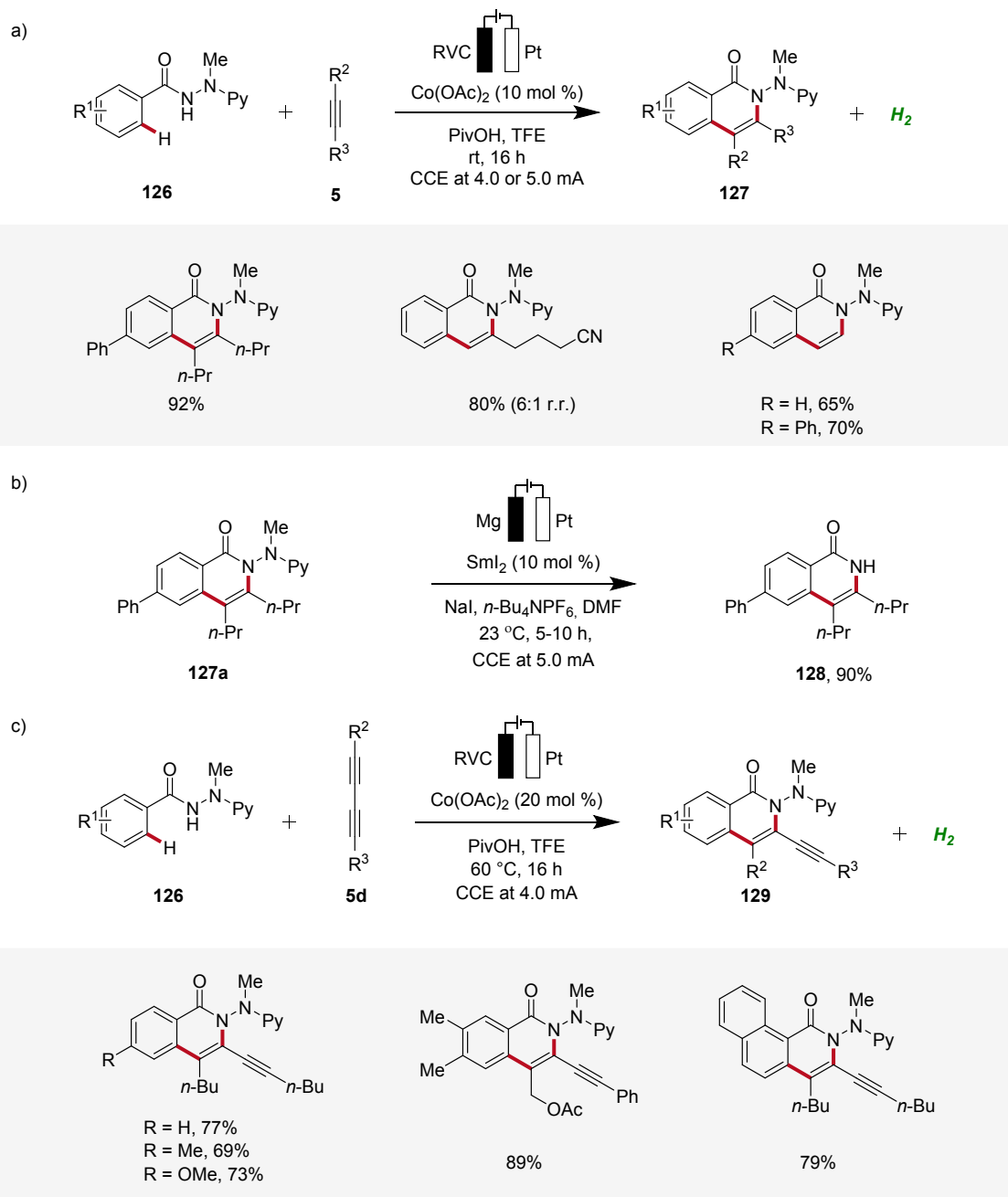


449

450 **Scheme 39:** Cobalt electro-catalyzed C–H/N–H ethyne annulation.

451 Furthermore, Ackermann demonstrated the applicability of cobalt electro-catalyzed C–H/N–H  
 452 alkyne annulation to benzamide **126** bearing an electro-removable *N*-2-pyridylhydrazone auxiliary  
 453 under exceedingly mild conditions at room temperature with ample scope (**Scheme 40a**).<sup>[49]</sup>  
 454 Interestingly, the auxiliary could be easily cleaved electro-reductive samarium-catalysis,  
 455 exhibiting the utility of this strategy (**Scheme 40b**).<sup>[49]</sup> In 2019, Ackermann further developed a  
 456 cobalt electro-catalyzed C–H/N–H annulation approach, specifically targeting the challenging  
 457 substrate class of 1,3-diyne **5d** (**Scheme 40c**).<sup>[50]</sup> The selectivity challenges associated with 1,3-  
 458 diynes **5d** are significantly more intricate compared to those observed with internal alkynes.  
 459 Remarkably, the developed approach demonstrated excellent substrate scope and significant  
 460 compatibility with various functional groups. Also here, the hydrazone directing group could be  
 461 easily cleaved through samarium-electrocatalysis.<sup>[50]</sup>





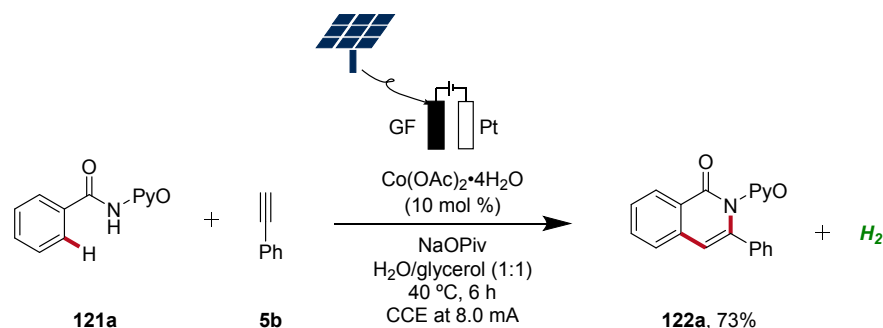
462

463 **Scheme 40:** Cobalt electro-catalyzed C–H/N–H annulations with electro-removable hydrazides464 **126.**

465



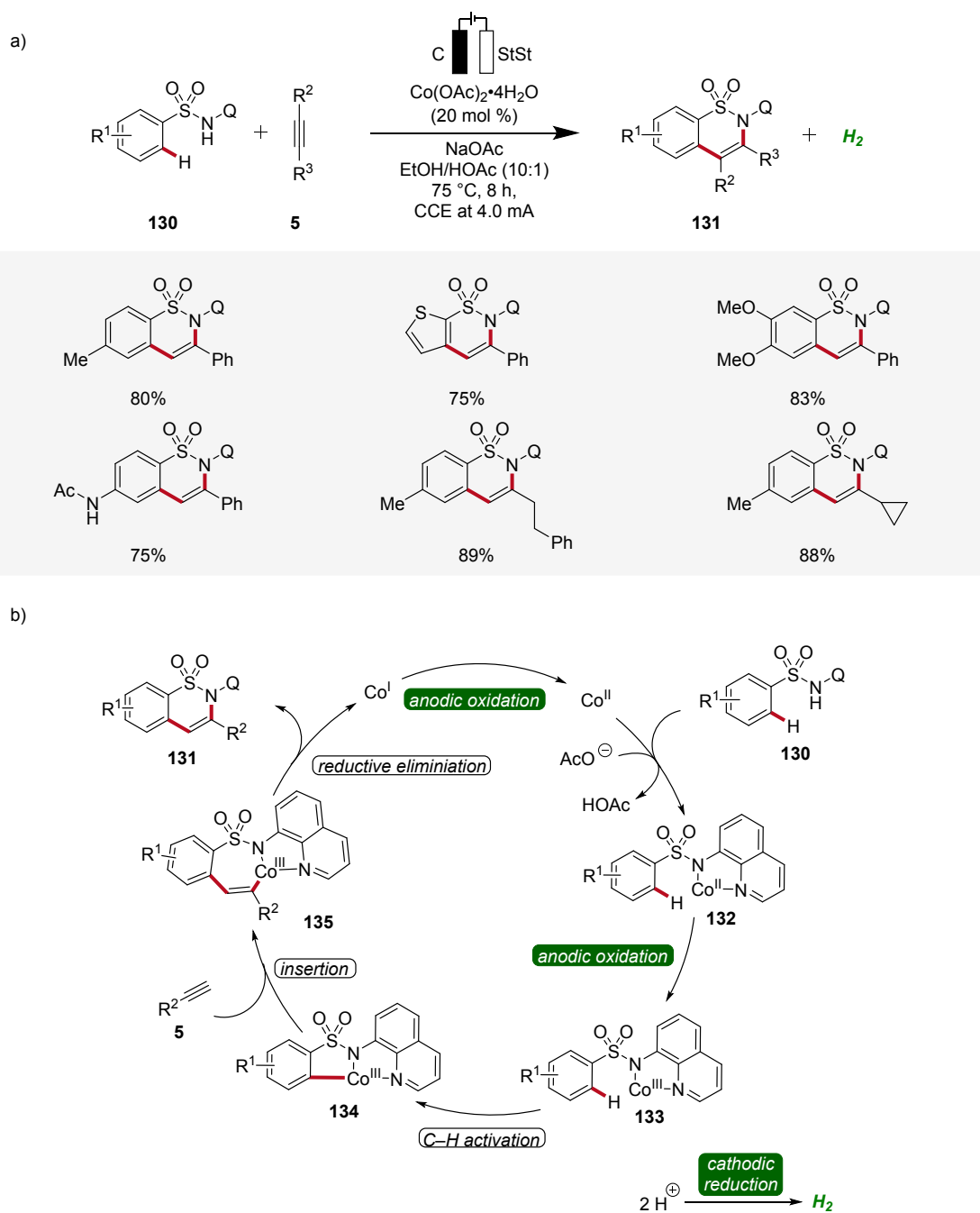
466 In 2020, Ackermann further demonstrated the green aspects of cobalt electro-catalyzed C–H  
 467 activation by performing the synthesis of isoquinolinones **122** in biomass-derived glycerol in an  
 468 user-friendly undivided cell under galvanostatic electrolysis.<sup>[51]</sup> Importantly, the direct use of  
 469 renewable energy sources, including sunlight and wind power, to drive this sustainable and  
 470 resource-economic electrocatalytic transformation was established, showcasing the robustness and  
 471 practicality (**Scheme 41**).<sup>[51]</sup>



473 **Scheme 41:** Cobalt electro-catalyzed C–H alkyne annulation in aqueous glycerol driven by  
 474 natural sunlight.

475 In 2020, Lei applied the cobalt-electrocatalysis strategy to synthesize structurally diverse sultams  
 476 **131** by the annulation of sulfonamides **130** with alkynes **5** (**Scheme 42**).<sup>[52]</sup> The reaction was  
 477 performed in an undivided cell under galvanostatic electrolysis. Various sulfonamides **130** and  
 478 alkynes **5** substituted with different functional groups were explored which delivered the broad  
 479 substrate scope of this method. Internal alkynes **5** also produced the annulation products in  
 480 moderate to high yields (**Scheme 42a**). Mechanistic studies revealed that first, the cobalt(II)  
 481 species is coordinated by the sulfonamide substrate **130** to produce the cobalt(II) complex **132**  
 482 which is oxidized to generate the cobalt(III) intermediate **133**. Next, the cyclometallated cobalt(III)  
 483 complex **134** is generated by C–H activation followed by insertion of alkyne **5**. Lastly, reductive  
 484 elimination leads to the final annulation product **131** (**Scheme 42b**).<sup>[52]</sup>





485

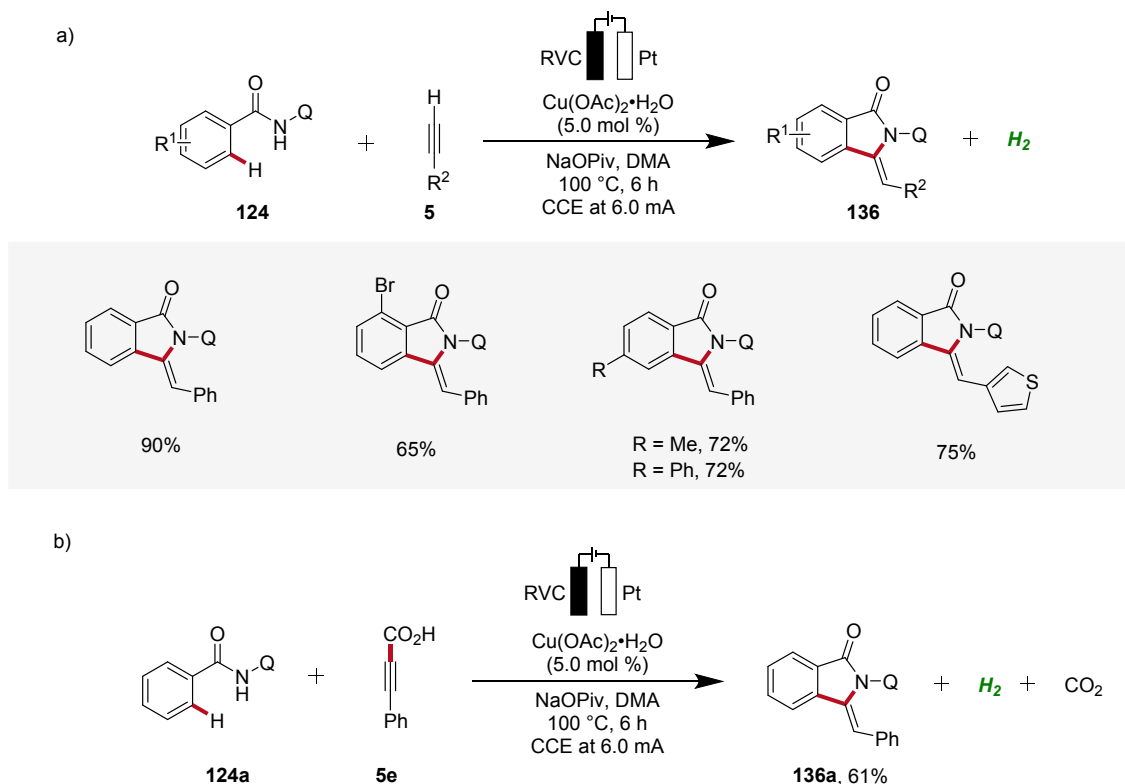
486 **Scheme 42:** Versatility and schematic catalytic cycle for the synthesis of sultams **131** via  
 487 cobalt electro-catalyzed C–H annulation.

488



489 **3.2 Cupraelectro-Catalyzed C–H Activation**

490 Copper plays a significant role in transition metal-catalysis being an Earth-abundant and cost-  
 491 effective transition metal with unique properties and versatility.<sup>[53]</sup> In 2019, Ackermann reported  
 492 on the first cupraelectro-catalyzed C–H activation (**Scheme 43**).<sup>[54]</sup> This resource-economic  
 493 strategy allowed for alkyne annulation with benzamides **124** and terminal alkynes **5** and exhibited  
 494 excellent functional group tolerance (**Scheme 43a**). Interestingly, the cupra-electrocatalysis led to  
 495 the formation of isoindolones **136**, rather than isoquinolones as observed under cobalta-  
 496 electrocatalysis.<sup>[46, 49]</sup> In addition, the strategy also allowed for decarboxylative C–H/C–C  
 497 functionalizations by electrocatalysis (**Scheme 43b**).<sup>[54]</sup>

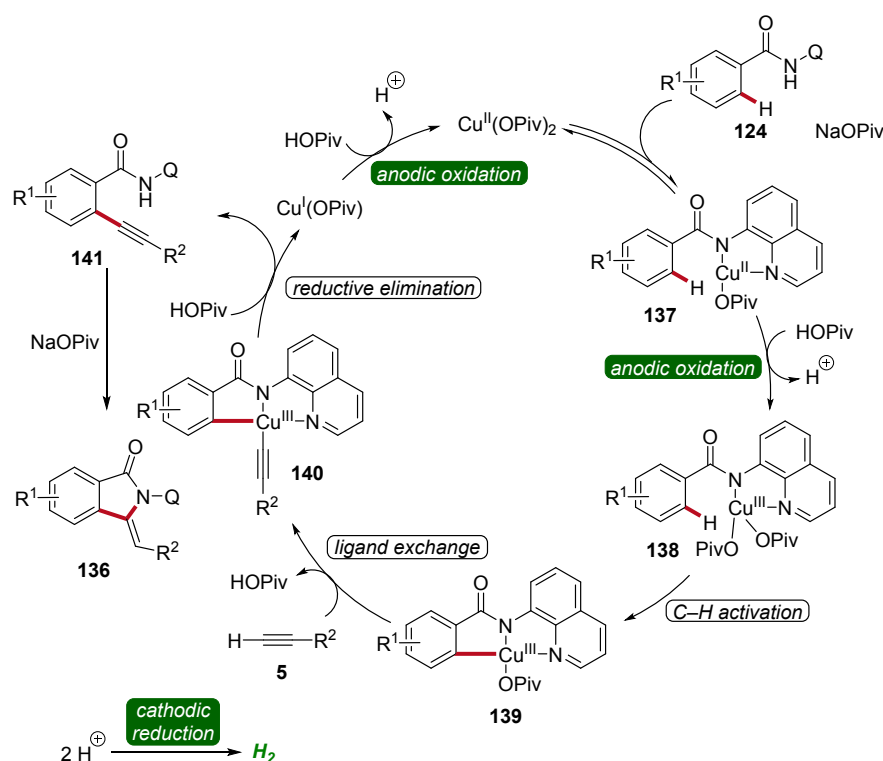


**Scheme 43:** Cupraelectro-catalyzed C–H alkyne annulations to construct isoindolones **136**.





501 Based on detailed mechanistic investigations, including H/D exchange experiments, kinetic  
 502 isotope effect studies, and *in-operando* kinetic analyses as well as cyclic voltammetry studies, a  
 503 plausible mechanism was described (**Scheme 44**). Hence, by coordination of the substrate **124** and  
 504 anodic oxidation, the formation of the copper(III) intermediate **138** is promoted. This species then  
 505 undergoes C–H activation to form the cupra(III)-cycle **140**, followed by metalation of the terminal  
 506 alkyne **5**. The subsequent reductive elimination delivers the C–H alkynylated arene **141**, which  
 507 undergoes cyclization to furnish the desired isoindolone product **136**. The copper(I) complex is  
 508 then oxidized at the anode to regenerate the catalytically active high-valent copper species  
 509 (**Scheme 44**).<sup>[54]</sup>



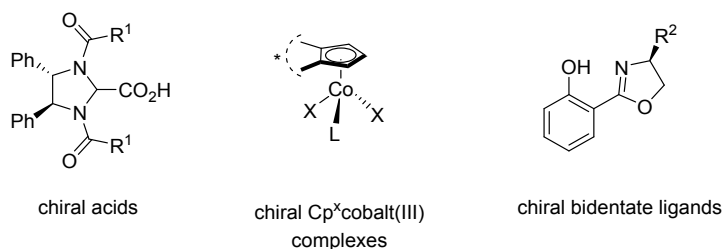
510

511 **Scheme 44:** Catalytic cycle for the cupraelectro-catalyzed C–H activation leading to isoindolones  
 512 **136**.



### 514 3.3 Enantioselective 3d Metallalectro-Catalyzed Alkyne Annulations

515 The 3d transition metal cobalt has recently emerged as a particularly promising catalyst for  
 516 enantioselective C–H activation.<sup>[55]</sup> Its low cost, abundant availability, and unique reactivity make  
 517 it an attractive alternative to the earlier established 4d and 5d transition metals such as palladium,  
 518 rhodium, and iridium. Hence, in the field of high-valent cobalt-catalyzed C–H activation, various  
 519 strategies for controlling enantioselectivity have been identified (**Scheme 45**).<sup>[56]</sup> In 2018,  
 520 Ackermann introduced newly designed C<sub>2</sub> symmetric chiral carboxylic acids to enable the first  
 521 examples of enantioselective high-valent cobalt-catalyzed C–H activation.<sup>[57]</sup> Later, in 2019,  
 522 Cramer identified chiral cyclopentadienyl cobalt(III) complexes as viable pre-catalysts for C–H  
 523 activation reactions with high enantioselectivity.<sup>[58]</sup> Subsequently, in 2022, Shi<sup>[59]</sup> and Niu<sup>[60]</sup>  
 524 applied chiral salicyloxazoline ligands, first described by Bolm<sup>[61]</sup>, for enantioselective cobalt-  
 525 catalyzed C–H activations employing bidentate directing groups.

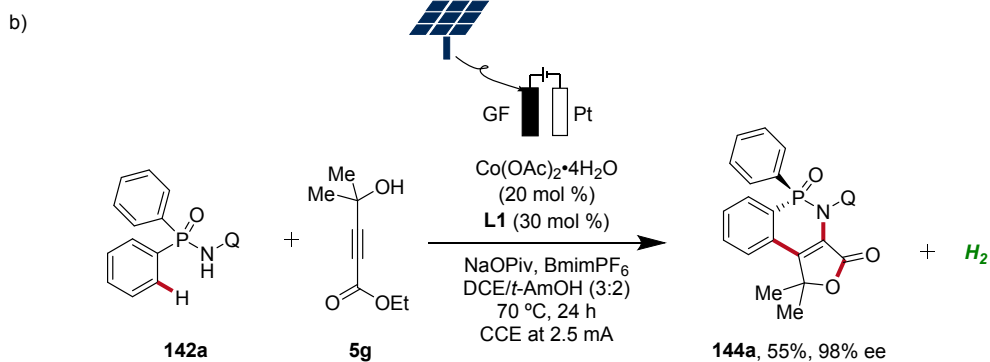
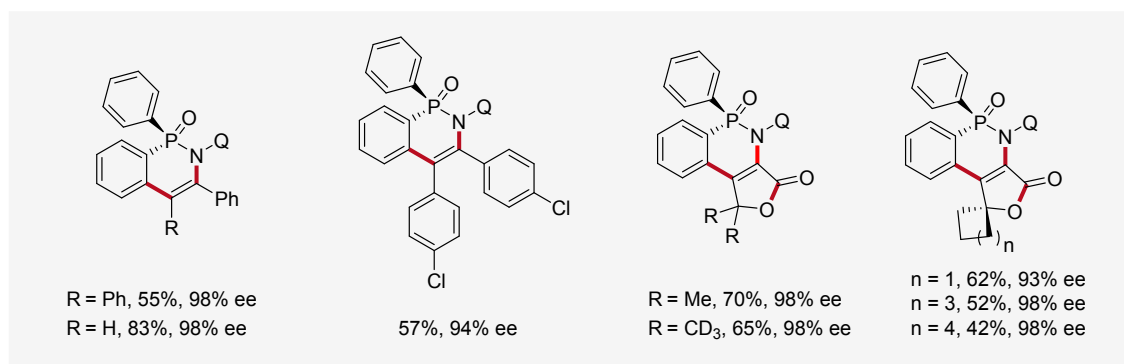
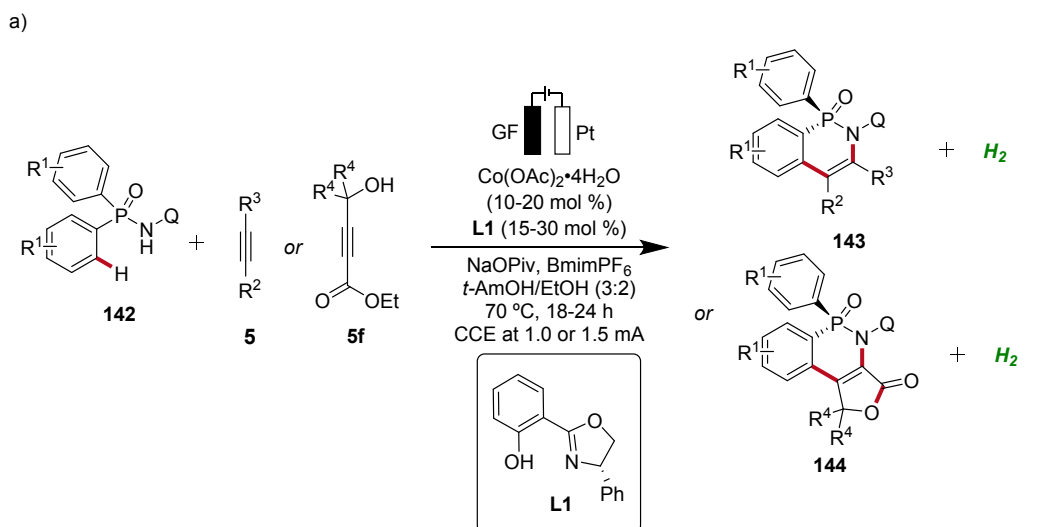


526

527 **Scheme 45:** Control of enantioselectivity in high-valent cobalt-catalyzed C–H activation.

528 In 2023, Ackermann delineated the first enantioselective cobaltalelectro-catalyzed C–H activations  
 529 (**Scheme 46**).<sup>[62]</sup> Employing **L1** as ligand, the enantioselective C–H annulation of arylphosphinic  
 530 amides **142** and alkynes **5** successfully yielded *P*-chiral cyclic phosphinic amides **143** with  
 531 exceptional enantioselectivity and broad substrate scope (**Scheme 46a**). Furthermore, the efficacy  
 532 of this transformation extends beyond conventional alkynes **5**, as the cascade annulation involving  
 533 alkynoates **5f** was also accomplished. Importantly, it could be demonstrated that the  
 534 enantioselective cobalta-electrocatalysis can directly be driven by natural sunlight as a renewable  
 535 form of energy using a solar-panel (**Scheme 46b**).<sup>[62]</sup>





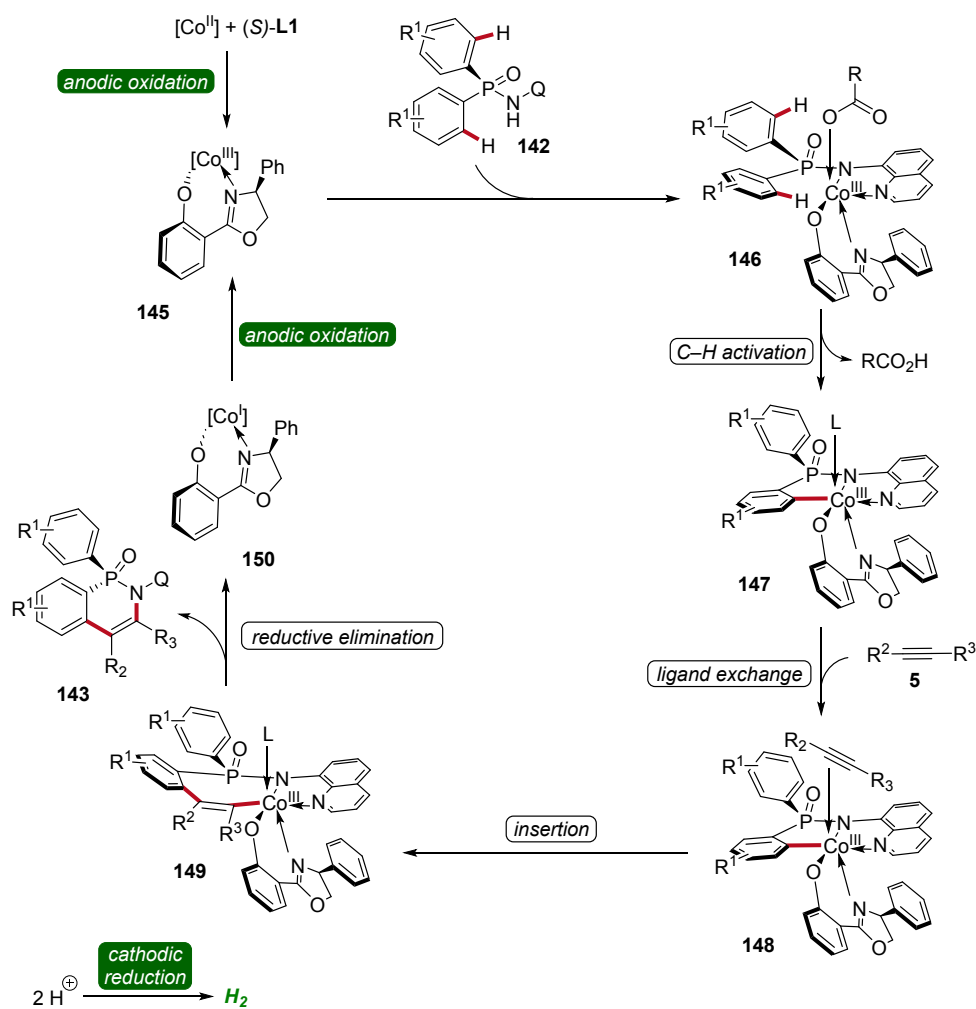
536

537 **Scheme 46:** Enantioselective cobalt-electrocatalyzed C–H alkyne annulations for the synthesis  
 538 of *P*-stereogenic compounds **143** and **144**.

539



540 Based on mechanistic studies and previous reports<sup>[47, 59, 62-63]</sup>, a reaction mechanism is depicted  
 541 (**Scheme 47**). First, anodic oxidation of the cobalt(II) pre-catalyst generates the active chiral  
 542 cobalt(III), which is coordinated by the chiral ligand **L1** and substrate **142** to form intermediate  
 543 **146**. Next, the cyclometallated cobalt(III) intermediate **147** is formed via enantioselective C–H  
 544 activation, followed by coordination and migratory insertion of alkyne **5**. Subsequent reductive  
 545 elimination delivers the chiral compound **143** along with cobalt(I) complex **150**. Finally, **150** is re-  
 546 oxidized by anodic oxidation to complete the catalytic cycle.

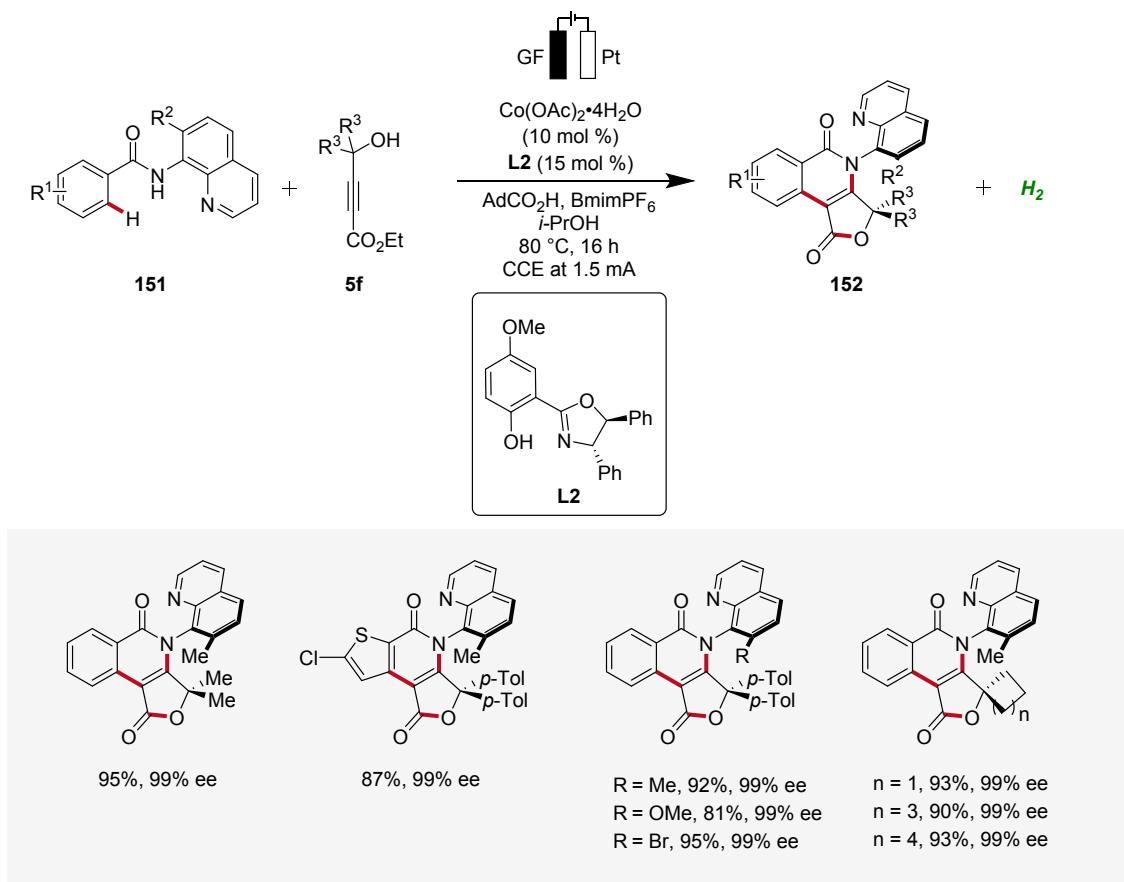


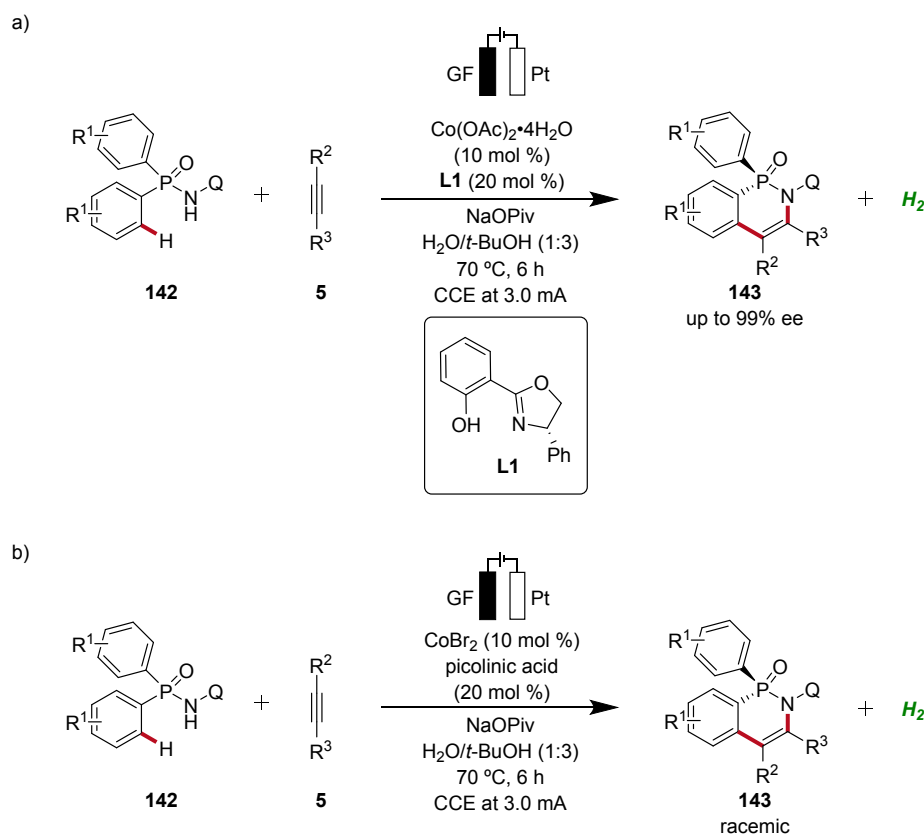
548 **Scheme 47:** Schematic catalytic cycle for the cobalt electro-catalyzed enantioselective C–H  
 549 annulation.

550 Moreover, Ackermann devised the first enantioselective cobalt electro-catalyzed synthesis of  
 551 axially chiral compounds **152** (**Scheme 48**).<sup>[62]</sup> The atropo-chiral products **152** were accessed with



552 excellent yields and enantiomeric purities. Notably, the atroposelective cobalta-electrocatalysis  
 553 proved to be scalable using cost-effective stainless steel as cathode material instead of the  
 554 commonly used precious platinum.<sup>[62]</sup>





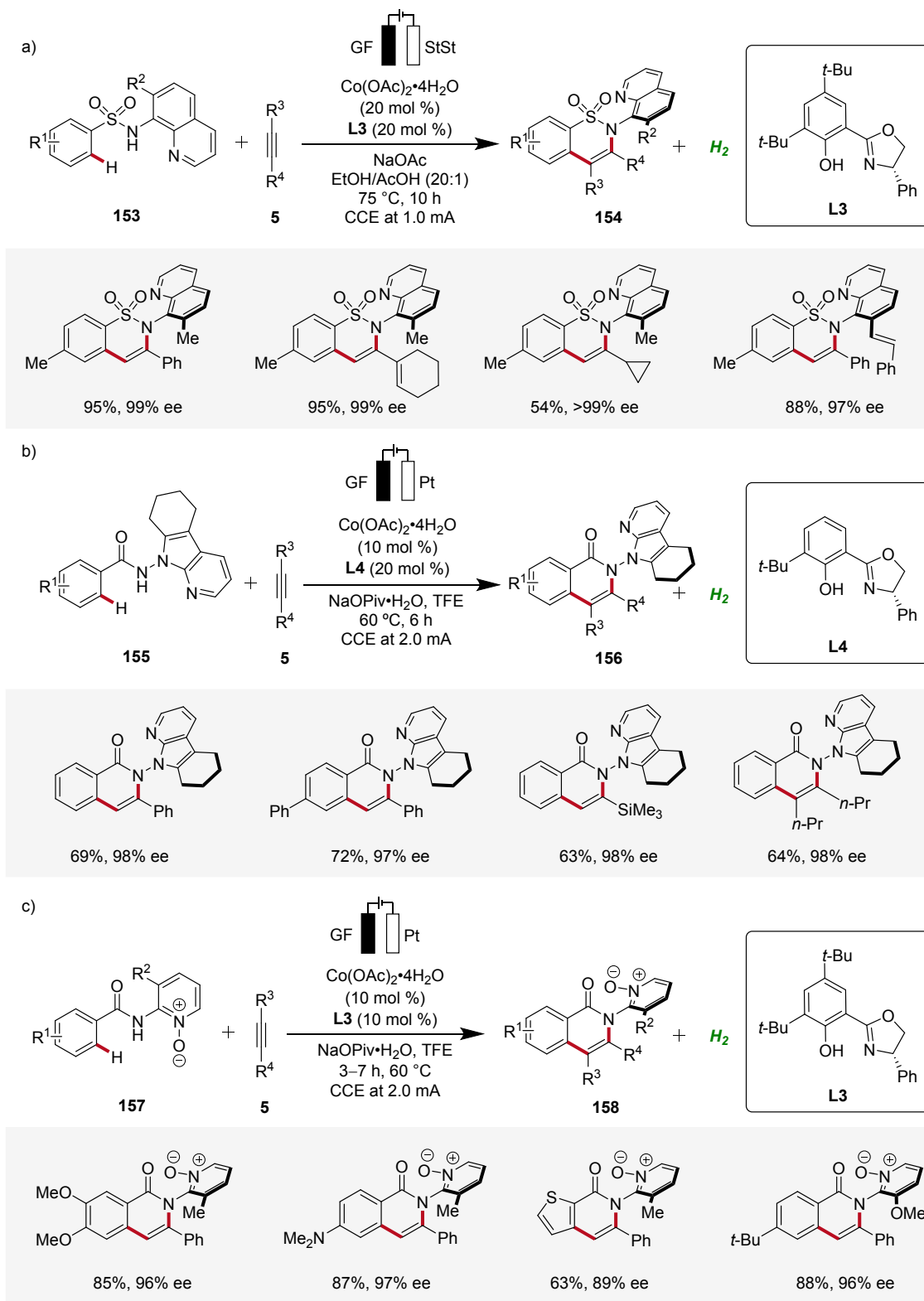
561

562 **Scheme 49:** Enantioselective and non-enantioselective cobalt electro-catalyzed C–H annulation  
 563 for the synthesis of *P*-stereogenic phosphinic amides **143**.

564 Furthermore, Niu contributed significantly demonstrating several cobalt electro-catalyzed  
 565 annulation reactions with alkynes for the assembly of axially chiral molecules using chiral salox-  
 566 based ligands (**Scheme 50**). First, an atroposelective annulation of alkynes **5** with sulfonamides  
 567 **153** was reported, forming atropo-chiral sultams **154** with high level of selectivity (**Scheme 50a**).  
 568 The strategy consisted a broad scope and high enantioselectivity in the products.<sup>[65]</sup> Later, Niu  
 569 devised an atroposelective annulation reaction with internal and terminal alkynes **5**, where 7-  
 570 azaindole derived directing groups were employed, leading to versatile *N–N* axially chiral  
 571 compounds **156** with high levels of enantioselectivity (**Scheme 50b**).<sup>[66]</sup> In addition, Niu reported  
 572 an atroposelective annulation of alkynes **5** employing benzamides **157** bearing pyridine-*N*-oxide  
 573 derived directing groups (**Scheme 50c**).<sup>[67]</sup>

574





575

576 **Scheme 50:** Atroposelective cobalt electro-catalyzed C–H annulations with diverse directing

577 groups.

54



## 578 4 Conclusion

579 The intersection of organic synthesis, renewable energy, and hydrogen economy through  
580 metallaelectro-catalysis reveals seminal opportunities towards sustainable development. Thus,  
581 electrocatalytic processes, powered by renewable forms of energy, can provide an alternative to  
582 traditional chemical methods, reducing the need for harsh reagents and minimizing waste.  
583 Importantly, pairing of organic synthesis to the valuable hydrogen evolution reaction (HER)  
584 enables a prospective integration into a decentralized green hydrogen economy.

585 Metallaelectro-catalysis, a rapidly evolving field, has emerged as a cutting-edge technique to forge  
586 new synthesis routes. Given that past research on C–H annulation reactions has primarily focused  
587 on precious transition metals, such as rhodium and ruthenium, it is anticipated that future efforts  
588 will increasingly emphasize more the Earth-abundant and less toxic transition metals. Hence, the  
589 commencing exploration of 3d transition metals, such as cobalt and copper, has paved the way for  
590 the development of resource-economical and environmentally benign processes. Moreover, the  
591 ability to control enantioselectivity, which is an essential feature in the synthesis of  
592 pharmaceuticals and agrochemicals, has very recently been accomplished and offers novel  
593 opportunities towards full selectivity control.

594 As electrocatalysis continues to advance, it is expected that this innovative technique will become  
595 an integral part of the toolkit of organic chemists. Its ability to redesign organic synthesis, coupled  
596 with its potential to be integrated into a decentralized green hydrogen economy, bodes well for a  
597 future in which electrocatalysis plays a central role in advancing sustainable chemical processes.





598 **Data availability**

599 No primary research results have been included and no new data were generated or analyzed as part of this  
600 review.

601

602 **Conflicts of interest**

603 There are no conflicts to declare.

604

605 **Acknowledgement**

606 The authors gratefully acknowledge support from the DFG (Gottfried Wilhelm Leibniz award)  
607 and the European Union's Horizon 2020 research and innovation program (ERC advanced grant  
608 agreement No. 101021358) to L.A.. Financial support of the Alexander von Humboldt Foundation  
609 to B.S. is gratefully acknowledged.



610 **References**

- 611 [1] a) W.-B. Shen, X.-T. Tang, *Org. Biomol. Chem.* **2019**, *17*, 7106-7113; b) L. Zheng, R. Hua, *Chem.*  
612 *Rec.* **2018**, *18*, 556-569; c) L. Yang, H. Huang, *Catal. Sci. Technol.* **2012**, *2*, 1099-1112; d) C.  
613 Janiak, *Coord. Chem. Rev.* **2006**, *250*, 66-94; e) Y. Zheng, W. Zi, *Tetrahedron Lett.* **2018**, *59*, 2205-  
614 2213; f) S. Hosseininezhad, A. Ramazani, *RSC Adv.* **2024**, *14*, 278-352; g) Y. Zhang, Z. Cai, S.  
615 Warratz, C. Ma, L. Ackermann, *Sci. China Chem.* **2023**, *66*, 703-724; h) A. Ramani, B. Desai, M.  
616 Patel, T. Naveen, *Asian J. Org. Chem.* **2022**, *11*, e202200047; i) J. P. Brand, J. Waser, *Chem. Soc.*  
617 *Rev.* **2012**, *41*, 4165-4179; j) H. C. Kolb, M. G. Finn, K. B. Sharpless, *Angew. Chem. Int. Ed.* **2001**,  
618 *40*, 2004-2021.
- 619 [2] a) K. M. Dawood, M. Alaasar, *Asian J. Org. Chem.* **2022**, *11*, e202200331; b) G. W. Gribble, *J.*  
620 *Chem. Soc., Dalton Trans.* **2000**, 1045-1075; c) I. Nakamura, Y. Yamamoto, *Chem. Rev.* **2004**,  
621 *104*, 2127-2198; d) Y. Yamamoto, *Chem. Soc. Rev.* **2014**, *43*, 1575-1600.
- 622 [3] S. Warratz, C. Kornhaas, A. Cajaraville, B. Niepötter, D. Stalke, L. Ackermann, *Angew. Chem.*  
623 *Int. Ed.* **2015**, *54*, 5513-5517.
- 624 [4] R. Mei, H. Wang, S. Warratz, S. A. Macgregor, L. Ackermann, *Chem. Eur. J.* **2016**, *22*, 6759-6763.
- 625 [5] A. G. Stamoulis, D. L. Bruns, S. S. Stahl, *J. Am. Chem. Soc.* **2023**, *145*, 17515-17526.
- 626 [6] P. M. Osterberg, J. K. Niemeier, C. J. Welch, J. M. Hawkins, J. R. Martinelli, T. E. Johnson, T. W.  
627 Root, S. S. Stahl, *Org. Process Res. Dev.* **2015**, *19*, 1537-1543.
- 628 [7] a) C. Ma, P. Fang, Z.-R. Liu, S.-S. Xu, K. Xu, X. Cheng, A. Lei, H.-C. Xu, C. Zeng, T.-S. Mei, *Sci.*  
629 *Bull.* **2021**, *66*, 2412-2429; b) L. Ackermann, *Acc. Chem. Res.* **2020**, *53*, 84-104; c) C. A. Malapit,  
630 M. B. Prater, J. R. Cabrera-Pardo, M. Li, T. D. Pham, T. P. McFadden, S. Blank, S. D. Minter,  
631 *Chem. Rev.* **2021**, *122*, 3180-3218.
- 632 [8] a) G. Chen, X. Li, X. Feng, *Angew. Chem. Int. Ed.* **2022**, *61*, e202209014; b) M. Ball, M. Weeda,  
633 *Int. J. Hydrog. Energy* **2015**, *40*, 7903-7919; c) J. A. Turner, *Science* **2004**, *305*, 972-974; d) J. O.  
634 M. Bockris, *Science* **1972**, *176*, 1323.
- 635 [9] a) P. Gandeepan, L. H. Finger, T. H. Meyer, L. Ackermann, *Chem. Soc. Rev.* **2020**, *49*, 4254-4272;  
636 b) R. Francke, R. D. Little, *Chem. Soc. Rev.* **2014**, *43*, 2492-2521; c) E. J. Horn, B. R. Rosen, P. S.  
637 Baran, *ACS Cent. Sci.* **2016**, *2*, 302-308; d) B. A. Frontana-Uribe, R. D. Little, J. G. Ibanez, A.  
638 Palma, R. Vasquez-Medrano, *Green Chem.* **2010**, *12*, 2099-2119; e) C. Zhu, N. W. J. Ang, T. H.  
639 Meyer, Y. Qiu, L. Ackermann, *ACS Cent. Sci.* **2021**, *7*, 415-431.
- 640 [10] a) K. Fagnou, M. Lautens, *Chem. Rev.* **2003**, *103*, 169-196; b) G. Song, F. Wang, X. Li, *Chem. Soc.*  
641 *Rev.* **2012**, *41*, 3651-3678; c) J. F. Roth, *Platin. Met. Rev.* **1975**, *19*, 12-14; d) S. Akutagawa, *Appl.*  
642 *Catal. A Gen.* **1995**, *128*, 171-207.
- 643 [11] Y. Qiu, W.-J. Kong, J. Struwe, N. Sauermann, T. Rogge, A. Scheremetjew, L. Ackermann, *Angew.*  
644 *Chem. Int. Ed.* **2018**, *57*, 5828-5832.
- 645 [12] W. J. Kong, L. H. Finger, A. M. Messinis, R. Kuniyil, J. C. A. Oliveira, L. Ackermann, *J. Am.*  
646 *Chem. Soc.* **2019**, *141*, 17198-17206.
- 647 [13] W. J. Kong, Z. Shen, L. H. Finger, L. Ackermann, *Angew. Chem. Int. Ed.* **2020**, *59*, 5551-5556.
- 648 [14] R. C. Samanta, L. Ackermann, *Chem. Rec.* **2021**, *21*, 1-13.
- 649 [15] Y. Wang, J. C. Oliveira, Z. Lin, L. Ackermann, *Angew. Chem. Int. Ed.* **2021**, *60*, 6419-6424.
- 650 [16] Y.-K. Xing, X.-R. Chen, Q.-L. Yang, S.-Q. Zhang, H.-M. Guo, X. Hong, T.-S. Mei, *Nat. Commun.*  
651 **2021**, *12*, 930.
- 652 [17] M. Stangier, A. M. Messinis, J. C. A. Oliveira, H. Yu, L. Ackermann, *Nat. Commun.* **2021**, *12*,  
653 4736.
- 654 [18] Z.-C. Wang, R.-T. Li, Q. Ma, J.-Y. Chen, S.-F. Ni, M. Li, L.-R. Wen, L.-B. Zhang, *Green Chem.*  
655 **2021**, *23*, 9515-9522.
- 656 [19] Y. Yuan, J. Zhu, Z. Yang, S.-F. Ni, Q. Huang, L. Ackermann, *CCS Chem.* **2022**, *4*, 1858-1870.
- 657 [20] P. P. Sen, R. Prakash, S. R. Roy, *Org. Lett.* **2022**, *24*, 4530-4535.
- 658 [21] C. Xu, Z. Zhang, T. Liu, W. Zhang, W. Zhong, F. Ling, *Chem. Commun.* **2022**, *58*, 9508-9511.



- 659 [22] S. L. Homölle, M. Stangier, E. Reyes, L. Ackermann, *Precis. chem.* **2023**, *1*, 382-387.
- 660 [23] a) T. Nishimura, *Chem. Rec.* **2021**, *21*, 3532-3545; b) Ł. Woźniak, J.-F. Tan, Q.-H. Nguyen, A.
- 661 Madron du Vigné, V. Smal, Y.-X. Cao, N. Cramer, *Chem. Rev.* **2020**, *120*, 10516-10543; c) J. F.
- 662 Hartwig, *Chem. Soc. Rev.* **2011**, *40*, 1992-2002.
- 663 [24] Y. Qiu, M. Stangier, T. H. Meyer, J. C. A. Oliveira, L. Ackermann, *Angew. Chem. Int. Ed.* **2018**,
- 664 *57*, 14179-14183.
- 665 [25] Q.-L. Yang, Y.-K. Xing, X.-Y. Wang, H.-X. Ma, X.-J. Weng, X. Yang, H.-M. Guo, T.-S. Mei, *J.*
- 666 *Am. Chem. Soc.* **2019**, *141*, 18970-18976.
- 667 [26] P. Saikia, S. Gogoi, *Adv. Synth. Catal.* **2018**, *360*, 2063-2075.
- 668 [27] Q.-L. Yang, H.-W. Jia, Y. Liu, Y.-K. Xing, R.-C. Ma, M.-M. Wang, G.-R. Qu, T.-S. Mei, H.-M.
- 669 Guo, *Org. Lett.* **2021**, *23*, 1209-1215.
- 670 [28] Q.-L. Yang, N.-N. Guo, S.-X. Liu, B.-N. Zhang, G.-D. Zou, D.-C. Wang, H. Wang, H.-M. Guo,
- 671 *Org. Chem. Front.* **2024**, *11*, 4849-4856.
- 672 [29] a) L. Ackermann, N. Hofmann, R. Vicente, *Org. Lett.* **2011**, *13*, 1875-1877; b) S. De Sarkar, W.
- 673 Liu, S. I. Kozhushkov, L. Ackermann, *Adv. Synth. Catal.* **2014**, *356*, 1461-1479; c) G. Duarah, P.
- 674 Kaishap, T. Begum, S. Gogoi, *Adv. Synth. Catal.* **2019**, *361*, 654-672; d) R. Gramage-Doria, C.
- 675 Bruneau, *Coord. Chem. Rev.* **2021**, *428*, 213602.
- 676 [30] Y. Qiu, C. Tian, L. Massignan, T. Rogge, L. Ackermann, *Angew. Chem. Int. Ed.* **2018**, *57*, 5818-
- 677 5822.
- 678 [31] F. Xu, Y.-J. Li, C. Huang, H.-C. Xu, *ACS Catal.* **2018**, *8*, 3820-3824.
- 679 [32] R. Mei, J. Koeller, L. Ackermann, *Chem. Commun.* **2018**, *54*, 12879-12882.
- 680 [33] M.-J. Luo, T.-T. Zhang, F.-J. Cai, J.-H. Li, D.-L. He, *Chem. Commun.* **2019**, *55*, 7251-7254.
- 681 [34] Z.-Q. Wang, C. Hou, Y.-F. Zhong, Y.-X. Lu, Z.-Y. Mo, Y.-M. Pan, H.-T. Tang, *Org. Lett.* **2019**,
- 682 *21*, 9841-9845.
- 683 [35] M.-J. Luo, M. Hu, R.-J. Song, D.-L. He, J.-H. Li, *Chem. Commun.* **2019**, *55*, 1124-1127.
- 684 [36] L. Yang, R. Steinbock, A. Scheremetjew, R. Kuniyil, L. H. Finger, A. M. Messinis, L. Ackermann,
- 685 *Angew. Chem. Int. Ed.* **2020**, *59*, 11130-11135.
- 686 [37] X. Tan, X. Hou, T. Rogge, L. Ackermann, *Angew. Chem. Int. Ed.* **2021**, *60*, 4619-4624.
- 687 [38] R. A. Sánchez-Delgado, M. Rosales, M. A. Esteruelas, L. A. Oro, *J. Mol. Catal. A Chem.* **1995**, *96*,
- 688 *231-243*.
- 689 [39] I. Choi, A. M. Messinis, X. Hou, L. Ackermann, *Angew. Chem. Int. Ed.* **2021**, *60*, 27005-27012.
- 690 [40] J. Rein, S. B. Zacate, K. Mao, S. Lin, *Chem. Soc. Rev.* **2023**, *52*, 8106-8125.
- 691 [41] a) U. Dhawa, C. Tian, T. Wdowik, J. C. A. Oliveira, J. Hao, L. Ackermann, *Angew. Chem. Int. Ed.*
- 692 **2020**, *59*, 13451-13457; b) U. Dhawa, T. Wdowik, X. Hou, B. Yuan, J. C. A. Oliveira, L.
- 693 Ackermann, *Chem. Sci.* **2021**, *12*, 14182-14188.
- 694 [42] Y.-Q. Huang, Z.-J. Wu, L. Zhu, Q. Gu, X. Lu, S.-L. You, T.-S. Mei, *CCS Chem.* **2022**, *4*, 3181-
- 695 3189.
- 696 [43] W. Wei, A. Scheremetjew, L. Ackermann, *Chem. Sci.* **2022**, *13*, 2783-2788.
- 697 [44] G. Zhou, T. Zhou, A.-L. Jiang, P.-F. Qian, J.-Y. Li, B.-Y. Jiang, Z.-J. Chen, B.-F. Shi, *Angew.*
- 698 *Chem. Int. Ed.* **2024**, *63*, e202319871.
- 699 [45] a) J. Bora, M. Dutta, B. Chetia, *Tetrahedron* **2023**, *132*, 133248; b) R. Mei, U. Dhawa, R. C.
- 700 Samanta, W. Ma, J. Wencel-Delord, L. Ackermann, *ChemSusChem.* **2020**, *13*, 3306-3356; c) M.
- 701 Moselage, J. Li, L. Ackermann, *ACS Catal.* **2016**, *6*, 498-525; d) G. Cahiez, A. Moyeux, *Chem.*
- 702 *Rev.* **2010**, *110*, 1435-1462.
- 703 [46] C. Tian, L. Massignan, T. H. Meyer, L. Ackermann, *Angew. Chem. Int. Ed.* **2018**, *57*, 2383-2387.
- 704 [47] T. H. Meyer, J. C. A. Oliveira, D. Ghorai, L. Ackermann, *Angew. Chem. Int. Ed.* **2020**, *59*, 10955-
- 705 10960.
- 706 [48] S. Tang, D. Wang, Y. Liu, L. Zeng, A. Lei, *Nat. Commun.* **2018**, *9*, 1-7.
- 707 [49] R. Mei, N. Sauermann, J. C. A. Oliveira, L. Ackermann, *J. Am. Chem. Soc.* **2018**, *140*, 7913-7921.
- 708 [50] R. Mei, W. Ma, Y. Zhang, X. Guo, L. Ackermann, *Org. Lett.* **2019**, *21*, 6534-6538.
- 709 [51] T. H. Meyer, G. A. Chesnokov, L. Ackermann, *ChemSusChem.* **2020**, *13*, 668-671.



- 710 [52] Y. Cao, Y. Yuan, Y. Lin, X. Jiang, Y. Weng, T. Wang, F. Bu, L. Zeng, A. Lei, *Green Chem.* **2020**,  
711 22, 1548-1552.
- 712 [53] a) S. E. Allen, R. R. Walvoord, R. Padilla-Salinas, M. C. Kozlowski, *Chem. Rev.* **2013**, *113*, 6234-  
713 6458; b) L. Liang, D. Astruc, *Coord. Chem. Rev.* **2011**, *255*, 2933-2945.
- 714 [54] C. Tian, U. Dhawa, A. Scheremetjew, L. Ackermann, *ACS Catal.* **2019**, *9*, 7690-7696.
- 715 [55] a) J. Loup, U. Dhawa, F. Pesciaioli, J. Wencel-Delord, L. Ackermann, *Angew. Chem. Int. Ed.* **2019**,  
716 58, 12803-12818; b) Ł. Woźniak, N. Cramer, *Trends Chem.* **2019**, *1*, 471-484.
- 717 [56] B. Garai, A. Das, D. V. Kumar, B. Sundararaju, *Chem. Commun.* **2024**, *60*, 3354-3369.
- 718 [57] F. Pesciaioli, U. Dhawa, J. C. A. Oliveira, R. Yin, M. John, L. Ackermann, *Angew. Chem. Int. Ed.*  
719 **2018**, *57*, 15425-15429.
- 720 [58] K. Ozols, Y.-S. Jang, N. Cramer, *J. Am. Chem. Soc.* **2019**, *141*, 5675-5680.
- 721 [59] Q.-J. Yao, J.-H. Chen, H. Song, F.-R. Huang, B.-F. Shi, *Angew. Chem. Int. Ed.* **2022**, e202202892.
- 722 [60] X.-J. Si, D. Yang, M.-C. Sun, D. Wei, M.-P. Song, J.-L. Niu, *Nat. Synth.* **2022**, 709-718.
- 723 [61] a) C. Bolm, K. Weickhardt, M. Zehnder, D. Glasmacher, *Helv. Chim. Acta* **1991**, *74*, 717-726; b)  
724 C. Bolm, K. Weickhardt, M. Zehnder, T. Ranff, *Chem. Ber.* **1991**, *124*, 1173-1180.
- 725 [62] T. von Münchow, S. Dana, Y. Xu, B. Yuan, L. Ackermann, *Science* **2023**, *379*, 1036-1042.
- 726 [63] a) Y. Lin, T. von Münchow, L. Ackermann, *ACS Catal.* **2023**, *13*, 9713-9723; b) T. Liu, W. Zhang,  
727 C. Xu, Z. Xu, D. Song, W. Qian, G. Lu, C.-J. Zhang, W. Zhong, F. Ling, *Green Chem.* **2023**, *25*,  
728 3606-3614.
- 729 [64] Z. Xu, W. Zhang, C. Xu, T. Liu, Z. Zhang, C. Zheng, D. Song, W. Zhong, F. Ling, *Adv. Synth.*  
730 *Catal.* **2023**, *365*, 1877-1882.
- 731 [65] X.-J. Si, X. Zhao, J. Wang, X. Wang, Y. Zhang, D. Yang, M.-P. Song, J.-L. Niu, *Chem. Sci.* **2023**,  
732 *14*, 7291-7303.
- 733 [66] T. Li, L. Shi, X. Wang, C. Yang, D. Yang, M.-P. Song, J.-L. Niu, *Nat. Commun.* **2023**, *14*, 5271.
- 734 [67] Y. Zhang, S.-L. Liu, T. Li, M. Xu, Q. Wang, D. Yang, M.-P. Song, J.-L. Niu, *ACS Catal.* **2024**, *14*,  
735 1-9.

736



No primary research results, software or code have been included and no new data were generated or analysed as part of this review.

[View Article Online](#)

DOI: 10.1039/D4CC03871A

